



**HAL**  
open science

## The power of imaging to understand extracellular vesicle biology in vivo

Frederik J Verweij, Leonora Balaj, Chantal M Boulanger, David R F Carter, Ewoud B Compeer, Gisela D'angelo, Samir El Andaloussi, Jacky G Goetz, Julia Christina Gross, Vincent Hyenne, et al.

### ► To cite this version:

Frederik J Verweij, Leonora Balaj, Chantal M Boulanger, David R F Carter, Ewoud B Compeer, et al.. The power of imaging to understand extracellular vesicle biology in vivo. *Nature Methods*, 2021, 18 (9), pp.1013-1026. 10.1038/s41592-021-01206-3. hal-03419832v1

**HAL Id: hal-03419832**

**<https://inserm.hal.science/hal-03419832v1>**

Submitted on 29 Sep 2021 (v1), last revised 9 Dec 2021 (v2)

**HAL** is a multi-disciplinary open access archive for the deposit and dissemination of scientific research documents, whether they are published or not. The documents may come from teaching and research institutions in France or abroad, or from public or private research centers.

L'archive ouverte pluridisciplinaire **HAL**, est destinée au dépôt et à la diffusion de documents scientifiques de niveau recherche, publiés ou non, émanant des établissements d'enseignement et de recherche français ou étrangers, des laboratoires publics ou privés.

# 1 The power of imaging to understand Extracellular Vesicle 2 biology in vivo

3 Frederik J. Verweij<sup>1,2</sup>, Leonora Balaj<sup>3</sup>, Chantal M. Boulanger<sup>4</sup>, David RF Carter<sup>5,27</sup>, Ewoud B  
4 Compeer<sup>6</sup>, Gisela D'Angelo<sup>7</sup>, Samir El Andaloussi<sup>8,27</sup>, Jacky G. Goetz<sup>9</sup>, Julia Christina  
5 Gross<sup>10</sup>, Vincent Hyenne<sup>9,11</sup>, Eva-Maria Krämer-Albers<sup>12</sup>, Charles P. Lai<sup>13</sup>, Xavier Loyer<sup>4</sup>,  
6 Alex Marki<sup>14</sup>, Stefan Momma<sup>15</sup>, Esther N.M. Nolte-'t Hoen<sup>16</sup>, Michiel D Pegtel<sup>17</sup>, Hector  
7 Peinado<sup>18</sup>, Graça Raposo<sup>7</sup>, Kirsi Rilla<sup>19</sup>, Hidetoshi Tahara<sup>20</sup>, Clotilde Théry<sup>21</sup>, Martin E. van  
8 Royen<sup>22</sup>, Roosmarijn Vandenbroecke<sup>23</sup>, Ann M. Wehman<sup>24</sup>, Kenneth Witwer<sup>25</sup>, Zhiwei Wu<sup>26</sup>,  
9 Richard Wubbolts<sup>16</sup>, Guillaume van Niel<sup>1,2</sup>.

10

## 11 Author information

12 **These authors contributed equally:** Leonora Balaj, Chantal Boulanger, David RF Carter,  
13 Ewoud B Compeer, Gisela D'Angelo, Samir El Andaloussi, Jacky G. Goetz, Julia C. Gross,  
14 Vincent Hyenne, Eva-Maria Krämer-Albers, Charles Lai, Xavier Loyer, Alex Marki, Stefan  
15 Momma, Esther Nolte 't Hoen, Michiel D Pegtel, Hector Peinado, Graça Raposo, Kirsi Rilla,  
16 Hidetoshi Tahara, Clotilde Théry, Martin E. van Royen, Roosmarijn Vandenbroecke, Ann M.  
17 Wehman, Kenneth Witwer, Zhiwei Wu, Richard Wubbolts

18 **These authors jointly directed this work:** Frederik J. Verweij and Guillaume van Niel.

## 19 Acknowledgements

20 The authors acknowledge financial support from the INCa 2019-125 (to FJV), the  
21 International Society for Extracellular Vesicles, the French Society of Extracellular vesicles,  
22 the Société Française des Microscopies, the ITMO BCDE for their support for the  
23 organization of the ISEV workshop Imaging EVs in vivo that provided the basis of this review.  
24 We thank Philip Stahl (Washington University School of Medicine, USA) for stimulating  
25 discussions and insight. EBC thanks M. Dustin for support through ERC AdG 670930. DRFC  
26 is supported by the BBSRC (BB/P006205/1) and Cancer Research UK (A28052). KR is  
27 supported by the UEF Cell and Tissue Imaging Unit, Biocenter Kuopio and Biocenter Finland  
28  
29  
30

## 31 Competing interests

32 FJV, LB, CMB, EBC, GD'A, JGG, JCG, VH, EMKA, CPL,XL,AM, SM, EN, MDP, HP, GR, KR,  
33 HT, CT, MEVR, RV, AMW, KW, ZW, GvN declare no competing interests. DRFC is  
34 employed by Evox Therapeutics Limited. SEA serves in the Scientific Advisory Board of  
35 EVOX Therapeutics  
36  
37

## 38 Additional information

39 Correspondence should be addressed to FJV ([frederikverweij@gmail.com](mailto:frederikverweij@gmail.com)) or GvN  
40 ([guillaume.van-niel@inserm.fr](mailto:guillaume.van-niel@inserm.fr)).

41

42

## 43 Reprints and permissions information

44

45

## 46 **Affiliations**

- 47 1. Université de Paris, Institute of Psychiatry and Neuroscience of Paris (IPNP), INSERM
- 48 U1266, F-75014 Paris, FR
- 49 2. GHU Paris Psychiatrie et Neurosciences, Hôpital Sainte Anne, F-75014 Paris, FR
- 50 3. Department of Neurosurgery, Massachusetts General Hospital, Harvard Medical School,
- 51 Boston, MA 02114, USA.
- 52 4. Université de Paris, PARCC, INSERM, Paris, FR
- 53 5. Oxford Brookes University, UK
- 54 6. Kennedy Institute of Rheumatology, NDORMS, University of Oxford, OX3 FTY, UK.
- 55 7. Institut Curie, PSL Research University, CNRS, UMR144 –Cell Biology and Cancer 75005,
- 56 Paris, FR.
- 57 8. Clinical Research Center, Department of Laboratory Medicine, Karolinska Institutet,
- 58 Stockholm, 17177, Sweden.
- 59 9. INSERM UMR\_S1109, Tumor Biomechanics Lab, Université de Strasbourg, Fédération de
- 60 Médecine Translationnelle de Strasbourg (FMTS).
- 61 10. Health and Medical University Potsdam, DE
- 62 11. CNRS SNC5055, F-67000 Strasbourg, FR
- 63 12. Johannes Gutenberg-Universität Mainz, Institute of Developmental Biology and
- 64 Neurobiology, DE
- 65 13. Institute of Atomic and Molecular Sciences, Academia Sinica, Taipei, TW
- 66 14. La Jolla Institute for Allergy and Immunology, La Jolla, CA, USA.
- 67 15. Institute of Neurology (Edinger Institute), Goethe-University, Frankfurt am Main, DE
- 68 16. Dept Biomolecular Health Sciences, Faculty of veterinary medicine, Utrecht University,
- 69 Utrecht, NL
- 70 17. Amsterdam UMC, Vrije Universiteit Amsterdam, Pathology, Cancer Center Amsterdam,
- 71 Amsterdam, NL.
- 72 18. Microenvironment and Metastasis Laboratory, Molecular Oncology Programme, Spanish
- 73 National Cancer Research Center (CNIO), Madrid, ES
- 74 19. University of Eastern Finland, Institute of Biomedicine, Kuopio, FI
- 75 20. Department of Cellular and Molecular Biology, Graduate School of Biomedical and Health
- 76 Sciences, Hiroshima University, Hiroshima, Japan.
- 77 21. Institut Curie, PSL Research University, INSERM U932, Immunity & Cancer, 75005, Paris,
- 78 FR
- 79 22. Erasmus MC, Department of Pathology, Rotterdam, NL
- 80 23. VIB Center for Inflammation Research, Ghent, BE.
- 81 24. Department of Biological Sciences, University of Denver, Denver, CO, USA
- 82 25. Department of Molecular and Comparative Pathobiology and Neurology and the
- 83 Richman Family Precision Medicine Center of Excellence in Alzheimer's Disease, Johns
- 84 Hopkins University School of Medicine, Baltimore, Maryland, USA.
- 85 26. Center for Public Health Research, Medical School, Nanjing University, Nanjing, China;
- 86 State Key Laboratory of Analytical Chemistry for Life Science, Nanjing University, Nanjing,

87 China; Medical School, Jiangsu Key Laboratory of Molecular Medicine, Nanjing University,  
88 Nanjing, China.  
89 27. Evox Therapeutics Limited, Oxford Science Park, Oxford, OX4 4HG, UK.  
90  
91

92 **ABSTRACT (150 max)**

93 Extracellular Vesicles (EVs) are nano-sized lipid bilayer vesicles released by virtually every  
94 cell type. EVs have diverse biological activities, ranging from roles in development and  
95 homeostasis to cancer progression, spurring the development of EVs as disease biomarkers  
96 and drug nanovehicles. Due to the small size of EVs, however, most studies have relied on  
97 isolation and biochemical analysis of bulk EVs separated from biofluids. These approaches  
98 do not capture the dynamics of EV release, biodistribution, and other contributions to (patho-  
99 )physiology. Recent advances in live and high-resolution microscopy techniques, combined  
100 with innovative EV labeling strategies and reporter systems, provide new tools to study EVs  
101 *in vivo* in their physiological environment and at the single-vesicle level. Here, we critically  
102 review the latest advances and challenges in EV imaging, and identify urgent, outstanding  
103 questions in our quest to unravel EV biology and therapeutic applications.

104

105 **INTRODUCTION**

106 Knowledge of extracellular vesicle (EV) biogenesis pathways and biological activities has  
107 grown rapidly in the last decade<sup>1</sup>. EVs are membrane-enclosed structures that are released  
108 into the extracellular milieu by all organisms and cell types studied so far. EVs comprise a  
109 diverse family in which subtypes have been defined based on (sub)cellular origin, size, and  
110 composition: endosome-derived vesicles - including multivesicular endosome-derived  
111 exosomes with a diameter of 50-150 nm and secretory autophagosome-derived EVs;  
112 microvesicles/ectosomes that bud from the plasma membrane (PM) as small as exosomes  
113 or up to several  $\mu\text{m}$  in size; midbody remnants released by dividing cells; migrasomes trailing  
114 behind migrating cells<sup>2,3</sup>; apoptotic bodies dislodged from dying and disintegrating cells; and  
115 large oncosomes released by transformed cells with exaggerated membrane plasticity  
116 (**Figure 1A, Table 1**). Recent discoveries reveal additional subclasses of micro- and  
117 nanoparticles, such as exophers<sup>4,5</sup>, exomeres<sup>6</sup>, supramolecular attack particles<sup>7</sup>, and  
118 elongated particles<sup>8</sup>. Initial discoveries implicated EVs in cellular adherence (as 'adherons')<sup>9</sup>  
119 and clearance<sup>10</sup> in the early 1980s, and in immune regulation in the mid-1990s<sup>11</sup>. EVs also  
120 play crucial roles in neurodegenerative diseases, cancer progression, metabolic  
121 homeostasis, angiogenesis, inflammation, neuronal plasticity, migration, trophic support, and  
122 pathogenic infections<sup>12-15</sup>. These roles are primarily supported<sup>12-15</sup> by the capacity of EVs to  
123 shuttle molecules from one cell to another.

124 Despite the clear importance of EV biology, EV research faces challenges imposed by the  
125 small size and heterogeneity of EVs. Most studies have used bulk separation and  
126 characterization of heterogeneous populations of EVs from biological fluids or extended,  
127 large-scale *in vitro* cell cultures. These approaches allow robust characterization<sup>16</sup> at the  
128 population level, e.g. size and molecular profiles, but removing EVs from their context

129 precludes insight into subcellular origin, release- and uptake dynamics, and half-life.  
130 Separation can also disrupt fragile components such as branched glycans, potentially  
131 altering EV functionality. Furthermore, 2D monocultures do not necessarily reflect the *in vivo*  
132 situation.

133  
134 Recent advances in live- and high-resolution microscopy, combined with novel EV labeling  
135 strategies, now allow us to interrogate the composition and behavior of EVs at the single-  
136 vesicle level in living organisms<sup>17-20</sup> (**Box 1**). Functional transfer of EV proteins and RNA can  
137 also be assessed with using novel reporters *in vivo*<sup>21,22</sup> and *in vitro*<sup>23</sup>. These developments  
138 open new vistas on EV biology, providing the means to address previously intractable issues  
139 such as assessing the lifespan of EVs *in vivo*. Here, we review the state-of-the-art in EV  
140 labeling and tracking in animal model systems. We identify pitfalls and propose solutions and  
141 best practices. Finally, we discuss how recent advances in imaging can address open  
142 questions in EV biology from biogenesis to uptake and function, thereby enhancing the  
143 development of EV therapeutics.

#### 144 145 **A. Tagging strategies, microscopy technology and animal models.**

146 EV imaging presupposes a suitable labeling strategy that supports sub-cellular resolution. In  
147 recent years, several novel strategies or applications were developed, ranging from novel  
148 lipid dyes to luminal dyes and genetic labeling (**Table 2 and Figure 1**).

##### 149 150 *Lipid dyes*

151 Lipid dyes (e.g. PKH67, DiR/DiD, MemGlow) have been widely applied to label EVs with  
152 various excitation/emission wavelengths<sup>24</sup>, including the infrared range for greater  
153 penetration through tissues for *in vivo* studies. However, the application of lipophilic dyes to  
154 study EVs is complicated by unbound dye, aggregate/micelle formation, promiscuous  
155 labeling of non-EV particles, and long half-life<sup>25</sup>. Labeling protocols should therefore limit dye  
156 concentrations during labeling, remove free dye after labeling, include appropriate controls  
157 (e.g. 'dye only' control in EV solvent), and consider using multiple differentially stained EV  
158 populations to demonstrate absence of dye transfer or vesicle aggregation after (co-  
159 )isolation<sup>26</sup>. Recently, MemGlow<sup>27</sup> was reported to be brighter and less prone to aggregate  
160 formation compared with traditional lipid dyes<sup>19</sup>.

161 Lipid dyes can be applied directly to producer cells followed by EV isolation<sup>19</sup>. However, it is  
162 unknown if cell labeling affects EV release or function, or equally labels EV subtypes. Lipid  
163 dyes might also affect membrane-membrane fusion, fluidity of membrane proteins,  
164 membrane stiffness and EV size<sup>28</sup>. Since the half-life of lipid dyes greatly exceeds that of  
165 EVs<sup>29,30</sup>, EV degradation after cellular uptake can be masked by recycling/distribution of

166 fluorescent dye. Lipophilic dye-labelling of EVs may thus be more reliable in short-term  
167 studies<sup>31</sup>.

168

#### 169 *EV-luminal dyes*

170 Dyes such as carboxyfluorescein diacetate succinimidyl ester (CFDA-SE) and calcein-AM  
171 label proteins in the EV lumen<sup>30,32</sup>. Their dependence on luminal esterases for conversion  
172 into a fluorescent product may produce fewer false-positive EV signals than lipophilic dyes  
173 but likely restricts labeling to a sub-population of esterase-containing EVs<sup>33</sup>.

174

#### 175 *Fluorescent and bioluminescent protein EV-reporters*

176 Various genetically encoded reporters have been developed to label all EVs or subtypes  
177 using fluorescence or bioluminescence. Labeled proteins expressed in the cytosol can be  
178 shuttled into the lumen of both exosomes and ectosomes (**Figure 1B**)<sup>22</sup>. Addition of a  
179 palmitoylation signal associates the reporter with the inner leaflet of PM-derived EVs *in vivo*  
180 (**Figure 1C**)<sup>34</sup>. For labeling of specific EV subtypes, reporters including GFPs, RFPs, or the  
181 bioluminescent ThermoLuc can be attached to EV cargos, e.g. syntenin or tetraspanin  
182 (TSPAN) family members (TSPAN4, CD63, CD81 and CD9)<sup>2,17,19,26,35</sup>, of which CD63 is most  
183 widely used. Alternative scaffolds and double labeling strategies<sup>36</sup> can be considered to  
184 permit subtype detection. In contrast to fluorescent proteins, bioluminescent proteins emit  
185 signal after substrate addition with a high signal-to-noise ratio but comparatively lower  
186 spatiotemporal resolution<sup>37</sup>. Therefore, bioluminescence-based reporters (gLuc-lactadherin,  
187 GlucB) are predominantly used in small animal models to track EV biodistribution at whole-  
188 animal and organ scales<sup>38,39</sup> (**Table 2**). More recently, a third category of EV reporter using  
189 bioluminescence resonance energy transfer (BRET) has been described (PalmGRET),  
190 allowing EV biodistribution analysis and *in vivo* quantification from whole animal to super-  
191 resolution without requiring multiple reporters<sup>40</sup>.

192

193 Excitingly, genetic labeling allows access to the entire fluorescent protein toolbox, including  
194 photo-switching and photo-activation, biosensors and bi-molecular fluorescent  
195 complementation. However, genetic labeling also comes with challenges. Labeling  
196 transmembrane proteins might disrupt conformation or cause steric hindrance of ligand-  
197 receptor interaction and organotropism<sup>41-43</sup>. EV surface-associated reporters may also be  
198 prone to proteolytic cleavage<sup>44</sup>, removing the signal<sup>45</sup>. Reporter overexpression may affect  
199 cellular signaling, EV cargo loading, or endogenous EV production and trafficking. While a  
200 recent study demonstrated that CD63-GFP labeling of EVs only minimally perturbed the EV  
201 proteome<sup>26</sup>, other studies reported alterations in endolysosomal trafficking<sup>46</sup>, suggesting  
202 context-specific effects. Overexpression may also misdirect the reporter protein to

203 unintended EV subtypes. Moreover, the amount of fluorescence emitted by the producing  
204 cell will ordinarily overpower the fluorescent signal of small (s)EVs (~ a millionth of the cell  
205 volume) in the immediate vicinity. One solution is the use of pH-sensitive fluorophores (e.g.  
206 pHluorin), which are quenched in acidic cellular organelles but detected upon EV release, as  
207 successfully applied *in vitro*<sup>47–50</sup> and *in vivo*<sup>17</sup> (**Figure 1D**). A second strategy is degran  
208 tagging, whereby cytosolic signal in the producing cell is degraded, while the signal in EVs  
209 persists<sup>51</sup> (**Figure 1E**).

210

#### 211 *Epitope targeting of EV surface proteins.*

212 EV-enriched surface proteins and glycans can be targeted to visualize and characterize EVs  
213 in live and fixed cells (**Figure 1F**). Pre-labeling of glycans on the PM with fluorescent  
214 hyaluronic acid binding complex (fHABC) allows live visualization of EV budding and fission  
215 from cell<sup>52</sup> surface. Fluorescently labelled antibody fragments, such as nanobodies or  
216 fragment antigen-binding (Fab) domains, can also target EV-enriched proteins, with the  
217 advantage of eliminating the need for a secondary antibody and their smaller size compared  
218 to intact immunoglobulins. These strategies are compatible with most microscopy  
219 approaches<sup>53</sup> and allow imaging at single-EV resolution<sup>54</sup>. With these tags, imaging EVs near  
220 the producing cells can be difficult if the epitope is present on both EVs and the PM.  
221 Depending on the resolute power of the imaging modality, the use of EV-capture<sup>55</sup> or  
222 immobilization strategies<sup>56</sup> may be necessary.

223

224 A 'one size fits all' EV reporter does not exist (yet), and a particular reporter should be  
225 chosen based on the biological question and available imaging equipment. The specificity of  
226 the labeling strategies to EVs should preferably be validated with super-resolution/ultra-  
227 structural techniques. Along these lines, several recent studies have used combinations of  
228 Correlative Light-Electron Microscopy (**CLEM**), Immuno-EM (IEM), and/or Scanning EM  
229 (SEM) to validate *in vitro* and *in vivo* approaches<sup>17,19,48,49</sup> (**Table 2**).

230

#### 231 *Microscopy*

232 Apart from successful labeling, live-imaging of EVs *in vivo* also requires a dedicated imaging  
233 set-up. Ideally, the set-up is suitable for deep tissue imaging while being resolute and  
234 sensitive enough to observe EVs without inducing phototoxicity (**Table 3**). This means relying  
235 on fast but often diffraction-limited systems. Although the small size of EVs does not prevent  
236 their detection by light-microscopy, insufficient structural detail is attained to determine EV  
237 diameter. The challenge for detecting EVs in the sub-200 nm range is to distinguish single  
238 EVs from EV clusters or dye/protein aggregates and other particles. Super-resolution  
239 microscopy (SRM), e.g., stochastic optical reconstruction microscopy (STORM) and photo-



240 activated localization microscopy (PALM), improve resolution to the nanometer scale, but  
241 often require fixation and are time-consuming. Other SRM approaches better suited for live-  
242 cell imaging of EV uptake and processing are structured illumination microscopy (SIM) and  
243 stimulated emission depletion microscopy (STED). All SRM techniques depend on high  
244 photon intensities, complicating detection of smaller EVs and increasing the risk of photo-  
245 bleaching and -toxicity, especially when imaging larger volumes *in vivo* over time. This  
246 renders some of the current SRM techniques incompatible with robust EV live-imaging *in*  
247 *vivo*.

248

249 What is the best fluorescence microscopy system to study EV biology? The answer depends  
250 on the specific research question and the physio/pathological context (**Table 3**). Confocal  
251 laser scanning microscopy (CLSM) can visualize EV uptake by living cells and dynamic  
252 intracellular distribution on a time scale of seconds. Multicolor imaging can determine the  
253 intracellular fate of individually labeled EVs in 3D. However, tracking of rapidly moving EVs  
254 (e.g. in circulation<sup>17,19</sup>) and/or longer-time lapses requires high-speed imaging with systems  
255 such as spinning disk- and selective plane illumination microscopy (SPIM). These set-ups  
256 allow fast acquisition of EV movement, image larger volumes *in vivo*, and limit  
257 photobleaching and phototoxicity<sup>57</sup>. However, cells might be negatively affected by  
258 illumination even before they start to display morphological changes such as membrane  
259 blebbing<sup>57,58</sup>. Subtle impacts of prolonged imaging, e.g. on cellular metabolic state, must be  
260 kept in mind since they might impact EV release quantitatively and/or qualitatively. Emerging  
261 techniques including lattice light-sheet microscopy (LLSM) could prove instrumental to  
262 enable sustained high resolution live imaging with minimal photobleaching and  
263 phototoxicity<sup>59</sup>.

264

265 (Immuno)EM/CLEM allows validation of EV-labeling approaches, e.g. to confirm proper  
266 association with intraluminal vesicles (ILVs)<sup>17,19,48,49</sup>. These approaches can be used in *in*  
267 *vitro* cultures and *in vivo* models to study aspects of the EV lifespan like extracellular fate  
268 post-secretion or subcellular distribution in receiving cells<sup>17,19,60</sup>. Importantly, EM provides  
269 ultrastructural resolution and label-free visualization of EVs in their native environment. In  
270 addition, immuno-labeling detects proteins at the single-EV/ILV level. However, (I)EM/CLEM  
271 is restricted to a *posteriori* imaging of fixed samples.

272

### 273 *Model organisms*

274 Molecular processes involved in EV biogenesis, secretion, and uptake can be studied as  
275 isolated processes using *in vitro* approaches. However, the physiological quantities, content,  
276 release dynamics, natural targets, and stability of EVs are likely impacted by the 3D

277 microenvironment. Especially when studying EVs in the context of intercellular  
278 communication, one of the main paradigms in the field, a relevant context is essential. The  
279 use of primary cell sources and 3D models is therefore arguably a much-needed step to  
280 provide more physiological relevance compared to 2D monocultures of immortalized cell  
281 lines *in vitro*.

282  
283 *D. melanogaster* is an attractive model system for studying EVs in tissue organization,  
284 development, and systemic crosstalk<sup>61,62</sup>. Wnt and Hh-containing EVs have been observed  
285 *ex vivo* in *D. melanogaster* wing imaginal discs<sup>63–65</sup>. In addition, *D. melanogaster* has been  
286 used to study EV biology during mating behavior and in adaptive immunity<sup>66</sup>. Recently, an  
287 EV subpopulation from Rab11-positive MVBs was shown to be evolutionary conserved in  
288 flies and human cells<sup>46</sup>.

289  
290 Imaging more complex tissues, however, comes with additional restraints (**Table 4 and**  
291 **Figure 2**). The smaller the observed particle, the more important optical accessibility of the  
292 surrounding tissue becomes to reduce noise. For instance, a chorioallantoic membrane  
293 (CAM) model system allows the visualization of CD63- and CD44-positive EVs *in vivo*<sup>48,67</sup>. In  
294 mice, functional EV cargo transfer from immune to neuronal cells and between tumor cells  
295 has been observed<sup>21,22</sup>, as well as stroma-glioblastoma interactions, including miRNA  
296 transfer<sup>18,68</sup>. Still, live-imaging of EVs in mice is currently restricted to larger EVs as small  
297 EVs likely escape detection in these models<sup>18</sup> and to tissues immediately adjacent to the  
298 imaging window<sup>18,22,69</sup> (**Figure 2B**). Imaging less accessible areas or across organs often  
299 requires organ extraction and *ex vivo* (post-fixation) analysis<sup>70</sup> and is possible only with  
300 sufficient EV accumulation over time. Moreover, sites of accumulation might not equate with  
301 sites of function. These considerations have complicated efforts to understand EV  
302 physiology.

303  
304 In Zebrafish (*D. rerio*) EVs can be tracked in the blood flow and throughout the embryo<sup>17,19</sup>,  
305 allowing continuous live-imaging of endogenous EVs and EVs exogenously administered to  
306 the embryo. This model has permitted the exploration of EV biology in unprecedented  
307 detail<sup>71</sup> (**Figure 2C and D**), revealing correlates of EV characteristics and function<sup>43</sup>. The  
308 worm *C. elegans* is similarly transparent and has been used to study inter-animal EV  
309 communication with fluorescently labeled EVs<sup>72</sup> and EV biogenesis mechanisms using the  
310 ultrastructural resolution of EM<sup>73,74</sup>.

311  
312 Importantly, the applicability of non-mammalian model systems to study human pathologies  
313 remains considerable: 82% of all disease-related genes are conserved in *D. rerio*, 75% in *D.*

314 *melanogaster*, and >65% in *C. elegans*<sup>75-77</sup>. For example, disease-related models of  
315 neurodegenerative pathologies and tumor development have been introduced over the past  
316 decade<sup>77,78</sup>. . While the degree of relevance to human physiology is certainly important, these  
317 considerations should emphatically not preclude important questions from being addressed  
318 and block the access to a superior level of insight altogether. *D. melanogaster*, *C. elegans*  
319 and *D. rerio* allow fundamental investigations in cell biology and development and are often  
320 vastly superior to murine models with regard to optical accessibility, genetic amenability,  
321 costs and suitability for medium- or high-throughput approaches (**Table 4**). For example,  
322 exogenous tagging of proteins and tissue-specific expression using gene traps is well  
323 established using the UAS/GAL4 system<sup>79</sup>. Various CRISPR/Cas9/12a systems are available  
324 for functional studies *in vivo*<sup>80,81</sup>, allowing loss/gain-of-function studies and endogenous  
325 tagging and live-imaging of proteins at endogenous expression levels (although these levels  
326 may not be sufficient to reliably follow small-sized particles such as EV). Thus, live-imaging of  
327 single EVs in *D. rerio*, CAM, *D. melanogaster* and *C. elegans* is highly realistic (**Figure 2 E**  
328 **and F**) in contrast with murine models. Additionally, these models can be used as “pre-  
329 mouse” models, where mice are subsequently deployed for key-validation steps. Such  
330 strategies are indeed consistent with the “3R” principles in animal research. Each model  
331 organism has its own strengths and weaknesses. The choice of model system should  
332 therefore depend on the research question, the necessary level of resolution (single vs bulk  
333 EVs), and the required throughput (**Table 4**).

334

## 335 **B. Imaging EV biogenesis, release and distribution**

336 *In vitro* studies revealed that most cells release EVs continuously and/or adapt release in  
337 response to triggers<sup>49,82,83</sup>. Similarly, most cells can take up EVs. Bulk EV isolation from  
338 culture media thereby neglects the subset of EVs that has been released and recaptured or  
339 does not spread beyond cell-cell interfaces. Moreover, culture media components and 2D vs  
340 3D culture methods significantly impact EV release and EV composition<sup>84-89</sup>. Furthermore,  
341 little is known about bulk or subtype EV release dynamics or its dependence on  
342 characteristics of specific tissues and conditions (growth, homeostasis, pathology, specific  
343 triggers). Live-imaging techniques now let us grasp these temporal, spatial, and conditional  
344 EV dynamics.

345

### 346 *Imaging EV Biogenesis and Release*

347 EVs have two main subcellular origins: intracellular compartments and the PM. While  
348 biogenesis at the PM is synonymous with release, release from intracellular compartments  
349 requires multiple steps, from ILV or autophagic vacuole biogenesis to organelle fusion with  
350 the cell surface for EV/exosome release (**Figure 1A**).

351 Recent developments have enabled live-visualization of PM-generated EVs by various  
352 approaches. Direct budding and fission of EVs into the extracellular milieu has been  
353 visualized in living cells after PM labeling with fHABC in various cell types<sup>52</sup> (**Figure 1C**).  
354 Lectins such as WGA have also been used to label the surface of migrating cells and detect  
355 the formation of migrasomes on retraction fibers<sup>90</sup>. Alternative approaches exploited  
356 migrasome-enriched transmembrane proteins such as TSPAN4 to live-track migrasome  
357 formation in migrating cultured cells and during embryonic development in *D. rerio*<sup>2,3,91</sup>.  
358 Fluorescently-tagged cytosolic proteins enriched in PM-derived EVs, such as midbody  
359 remnants, can also be harnessed to track biogenesis and uptake<sup>20,92</sup>. Immune cell synaptic  
360 microvesicle release can be studied on planar-supported lipid bilayers containing  
361 fluorescently-labelled triggers of cargo loading into EVs via CLEM and STORM  
362 techniques<sup>53,54</sup>. These approaches may allow study of the molecular machinery of EV  
363 generation in an ideal setting for super-resolution microscopy.

364  
365 To visualize exosome release, one key approach is to image MVB-PM fusion. The acidic  
366 late-endosomal pH means that PM fusion results in a burst of fluorescence from (super  
367 ecliptic) CD63-pHluorin<sup>93</sup>, which can be observed by live microscopy<sup>47,49,50</sup>. This approach  
368 depends on fast acquisition times or dynamic CLEM to distinguish full MVB-PM fusion from  
369 rapid kiss-and-run motions that are inefficient in exosome release<sup>49</sup> (**Figure 1D**). CD63-  
370 pHluorin provides single-cell spatial information of release and high temporal  
371 resolution<sup>47,49,50</sup>. But this approach is mostly suited for flat surfaces (e.g. the baso-lateral side  
372 of cells) and shorter time acquisitions at single-cell level, and hence less suitable than  
373 luciferase-coupled CD63 for medium- and high-throughput screens of EV biogenesis  
374 modulators<sup>94</sup>. Dual-color microscopy of dual-tagged reporters (pHluorin-CD63-mScarlet)  
375 allows MVBs to be tracked before fusion<sup>48</sup>, while other reporter combinations can unravel the  
376 molecular identity of MVBs that fuse with the PM<sup>50</sup>. However, using CD63-pHluorin to  
377 visualize MVB-PM fusion remains challenging *in vivo* due to the lack of high-speed and high-  
378 resolution modalities with limited phototoxicity<sup>17</sup>.

379 Imaging exosome/ILV formation in MVBs is equally challenging, as most live approaches  
380 lack single vesicle resolution. The induction of enlarged endosomes by overexpressing  
381 GTPase-defective Rab5 improves resolution, but alters MVB maturation and function<sup>95</sup>.  
382 Moreover, MVBs may be destined for lysosomal degradation rather than EV secretion,  
383 limiting their relevance for exosome biogenesis. The giant secretory MVB-like compartments  
384 from *D. melanogaster* accessory glands allow unperturbed confocal and super-resolution  
385 visualization of intracellular sorting events and colocalization analysis of fluorescently-  
386 labelled cargo proteins on ILVs *in vivo*<sup>46</sup>, but these processes may be particular to  
387 specialized cells.

388 Future developments are needed to combine measurements of ILV generation, exosome  
389 release, and PM budding simultaneously, e.g., using high-speed 3D imaging. A clever  
390 approach to visualize protein trafficking has already revealed differences in endosome- and  
391 PM-derived EV proteomes<sup>96</sup>. Understanding these processes in further detail will let us  
392 interfere with formation and/or release of EV subclasses and provide an invaluable asset in  
393 our quest to attribute specific functions to EV subtypes *in vivo*.

#### 394 395 *Imaging EV distribution*

396 After EV release *in vivo*, the microenvironment plays a major role in EV distribution and  
397 function. Apart from EV-intrinsic factors (e.g. adhesion molecules), the local 3D architecture,  
398 extracellular matrix (ECM)<sup>97</sup> and biological barriers between organs affect EV diffusion and  
399 influence the physiological role of EVs (**Figure 2A**). Since these constraints determine local  
400 retention<sup>47,98</sup> vs distant transport and may not be fully recapitulated *in vitro*, the need for  
401 realistic *in vivo* models of EV distribution is clear (**Figure 2**).

402 While murine studies are limited mostly to organ scale<sup>26</sup> and disclose only the ‘final  
403 destination’ of EVs, smaller, transparent organisms allow subcellular resolution<sup>19</sup> and live-  
404 tracking of EV diffusion and transport (**Table 4**). Bioluminescent-, radio- and metabolic-  
405 labelling are compatible with the former strategy, whereas the latter typically employs  
406 fluorescent protein- and lipid-labeling strategies.

407  
408 Compared with studying endogenous EVs, isolation and injection of exogenous EVs permits  
409 fine control of engineering and dosing for optimal half-life and functional<sup>43</sup> studies. Such  
410 studies have suggested rapid removal by tissue and cell types with sustained phagocytic  
411 capacity, even within five minutes of injection<sup>99</sup>. While EV injection does not recapitulate the  
412 earliest aspects of the EV life-span, two recent *in vivo* studies demonstrated that pre-labeled  
413 injected (tumor) EVs did not deviate considerably in fate from (physiological) EVs that are  
414 endogenously released in the blood flow<sup>17,19</sup> (**Figure 2C and D**).

415 Yet, it is not clear whether these examples are sufficient to warrant a generalized verdict  
416 concerning all EVs and all aspects of EV biology especially regarding mRNAtransfer<sup>100</sup>.  
417 Indeed, exogenous administration incompletely mimics physiological EV release levels  
418 (unless approximated by sustained delivery methods<sup>101</sup>), and physio/pathological factors that  
419 might influence endogenous EV subset(s) might be absent *in vitro*<sup>84–89</sup>. EV subtypes (co-  
420 )isolated from *in vitro* cultures, some of which would normally act locally, would also  
421 artificially reach non-physiological sites upon injection *in vivo*. For example, EVs involved in  
422 ECM deposition and modulation<sup>47,102</sup> might normally act near the cell of origin, as would EVs  
423 released at immunological or neurological synapses<sup>35,53,103,104</sup>. In addition, anatomical  
424 differences in vascular permeability (e.g. liver *versus* brain), pathological conditions affecting

425 endothelial barrier function, or antiviral mechanisms restricting EV diffusion could alter the  
426 efficiency of EV propagation and uptake<sup>99,105</sup>. Imaging the release and biodistribution of  
427 endogenous EV subsets *in vivo* under various conditions will reveal how EVs cross biological  
428 barriers under physiological conditions, for which only indirect proof is currently available,  
429 e.g., intravenously injected EVs in the brain<sup>106,107</sup>. Ultimately, comparative studies of both  
430 endogenous and exogenous EV administration are needed. Studying endogenous EVs will  
431 show physiological concentrations and dynamics of EV release and biodistribution that  
432 highlight the best sites and frequencies of injection. This will help us interpret exogenous EV  
433 studies and permit finer control of certain EV-intrinsic variables. Together, these comparisons  
434 will inform EV targeting approaches for therapeutics.

435

### 436 **C. Imaging interaction/uptake of EVs by recipient cells and related functions.**

437 The EV lifespan is often depicted as cell A releasing EVs that reach cell B, where  
438 endocytosis and (intraluminal) cargo delivery trigger a phenotypic response. While this  
439 communication paradigm is exciting and supported by literature, EVs can also act in an  
440 autocrine fashion or have other 'delivery-independent' extracellular functions such as ECM  
441 modulation, PM receptor engagement or transfer of EV-resident membrane proteins to  
442 recipient cells<sup>108–110</sup>. (**Figure 3A**).

443

#### 444 *Imaging interaction of EVs with recipient cells*

445 EVs can function by engaging PM-localized receptors at the target cell membrane, such as in  
446 antigen presentation, as super-cytokines, or as carriers of morphogens and ligands for  
447 pattern recognition receptors<sup>42,54,63,108,111–113</sup>. Whereas uptake of EVs has been amply  
448 demonstrated by (live) imaging, visualization of EV interaction with the PM has been reported  
449 on just a few occasions<sup>60</sup>, and only recently with live-imaging *in vitro*<sup>59,114</sup> and *in vivo*<sup>17,19</sup>.  
450 Currently limited direct observation<sup>115</sup> might owe to a lack of suitable reporters. Indeed,  
451 whereas most studies adding labeled EVs to target cells show intracellular accumulation  
452 rather than PM labeling, this does not preclude previous EV-PM interaction, especially since  
453 functional cargo delivery appears to be a rare event from the 'bulk EV flow' perspective. For  
454 certain EVs, uptake might indeed be a pre-requisite to function, but for other EVs, uptake  
455 followed by degradation could rather reflect an end-of-life event after signaling through PM  
456 receptors. To date, most reporter systems for EV function are focused on cytoplasmic cargo  
457 delivery rather than signal induction. Understanding fusion-independent EV functions thus  
458 requires combined microscopy approaches, such as CLEM (**Figure 3B**), *in vitro*<sup>35,60,113</sup> and *in*  
459 *vivo*<sup>17,19,61</sup> to cover the full range from whole organism to subcellular at sufficient resolution  
460 with light-microscopy or EM ultrastructural resolution.

461

#### 462 *Imaging cellular uptake of EVs*

463 EVs are widely reported to deliver contents into the cytoplasm of recipient cells such as  
464 signaling proteins, RNA binding proteins, genetic material, metabolites and enzymes.  
465 However, we know little about the fusion events or transporter systems necessary for such  
466 delivery. Often, studies follow uptake in bulk, lacking the resolution to study single-EV fate.  
467 Recently, EM has been used to examine EV uptake *in vivo*<sup>17,19</sup>. Live imaging approaches can  
468 reveal other details of EV fate, such as acidification of EV-containing compartments after  
469 uptake *in vitro*<sup>48</sup> and *in vivo*<sup>17</sup>, distinguishing “storage” from degradation (**Figure 3C**). V-  
470 ATPase inhibitors might be required if uptake and degradation are highly efficient in target  
471 cells or to facilitate detection of rare events. Note that the choice of dye (e.g. lipid or genetic  
472 protein labeling) determines what is being followed after EV uptake. Over time, labels might  
473 no longer represent intact EVs, but rather trafficking of the label itself or of lipid/protein  
474 fragments.

475

#### 476 *Imaging EV function in recipient cells*

477 EVs elicit phenotypic responses in proximally and distally located cells. Reporter systems  
478 have been developed to visualize transfer of mRNAs<sup>21,22,100</sup>, miRNAs<sup>39,116</sup>, shRNAs<sup>23</sup> and  
479 proteins<sup>117</sup>. Cytoplasmic delivery presupposes endosomal escape by EV-endosome fusion to  
480 avoid lysosomal degradation of EV cargos. So far, detection of cargo transfer by live-imaging  
481 is limited to induction of a global signal at the cellular scale (**Figure 3D**). Further resolution is  
482 needed to locate and elucidate endosomal escape, demanding new technological  
483 developments for single-molecule cargo tracking and to observe potential fusion of  
484 endocytosed EVs with the host membrane. Interestingly, *in vivo* mouse studies indicate that  
485 cargo transfer occurs at low ‘efficiency’ in the absence of a specific stimulus<sup>21,100</sup>. However,  
486 in certain pathological models, the functional uptake of EVs can be higher<sup>118</sup>, highlighting the  
487 need to study pathological situations in model organisms.

488

489 Several reports indicate a trophic support function of EVs via lysosomal degradation<sup>17,119</sup>.  
490 Lysosomal targeting can be studied by EM<sup>17,19</sup> (**Figure 3E**) or by live-imaging using EV  
491 reporters with different acid sensitivity<sup>20,120</sup>. Live-imaging *in vivo* revealed rapid internalization  
492 and degradation of injected or endogenous EVs by professional phagocytes (e.g.  
493 macrophages and monocytes) and especially pinocytes (e.g. scavenger endothelial cells).  
494 Some EVs might thus function without message delivery<sup>17,19</sup>. While trophic function is not  
495 strictly incompatible with ‘message transfer’, a yet-unresolved question is whether EV-  
496 mediated communication is stochastic or deterministic from a donor cell perspective. Do cells  
497 release a large amount of EVs agnostically, letting the recipient cell determine whether to

498 respond via an 'activation status' that determines cytoplasmic cargo delivery<sup>118</sup>? Or do cells  
499 release a limited number of "magic bullet" EVs that are tailored for specific communication?  
500 The latter is currently supported in the immunological synapse setting<sup>35,53,60</sup>, but is perhaps  
501 less evident beyond this close cell-cell contact setting. These 'magic bullets' might be  
502 present within the main flow but possess molecular traits that promote capture, facilitate  
503 back-fusion, or prevent degradation. Thus, tracking bulk EV flow may divert our attention  
504 from the rare EV-target cell interactions, the 'magic bullets' that do not follow bulk flow.

505

506 Technological strategies are important to monitor events in the transfer process<sup>121</sup>, but  
507 perhaps the most pressing need is to develop more fundamental knowledge of rare, "magic-  
508 bullet" events. When we know the players, we can image the co-packaging of cognate  
509 molecules and targeting molecules into ILVs/EVs to follow EV lifespan events in real time,  
510 from biogenesis to target cell interactions.

511

## 512 **Conclusion/Discussion**

513 Imaging technology has matured to the point where we can study most details of the EV  
514 lifespan *in vivo* using diverse tags and microscopy approaches, especially in optically  
515 transparent organisms. What is at stake is profound. Imaging biogenesis will distinguish EV  
516 subpopulations perhaps associated with distinct functions, and enable a firm nomenclature.  
517 By following the biodistribution of EVs *in vivo*, we will not only assess their capacity to cross  
518 biological barriers but also gain insight into their range of actions and their efficiency in  
519 reaching target cells previously identified *in vitro*. *In vitro* technologies can then be utilized to  
520 dissect mechanisms in more detail, lifting the veil around the important events that *in vivo*  
521 imaging has started to reveal<sup>69,106,122</sup>.

522 How EVs act as mediators of intercellular signaling is poorly understood. By following the  
523 fate of EVs *in vivo*, we will gain insight into their *in vivo* targets and functions. Direct imaging  
524 of the release of EV contents into recipient cells is needed to identify whether cargo transfer  
525 or signaling interaction (or both), is responsible for the effects of EVs. While most studies  
526 focus on EV functions requiring EV uptake and cargo transfer into recipient cells, mounting  
527 evidence points towards extracellular roles for EVs involving neither uptake nor cargo-  
528 delivery<sup>42,63,108,111,112,123</sup>. It is unclear how common extracellular vs. intracellular functions are  
529 *in vivo*, and whether EVs mainly act systemically vs. locally. The rapid clearance of the  
530 majority of injected EVs by the liver and spleen might indicate that many EVs function in  
531 waste disposal or trophic support. Therefore, it is important to determine the route taken by  
532 endogenous EVs *in vivo* and the amount of EVs necessary to impact target tissues.  
533 Following specific subclasses of EVs *in vivo* will aid in addressing these key questions, and



534 reveal whether EV communication is stochastic and inefficient or rather relies on specialized  
535 EVs to transfer messages.

536 Knowing the *in vivo* characteristics of EVs, such as their half-life, biodistribution and targeting  
537 mechanisms, also supports their clinical application as biomarkers, drug carriers, or intrinsic  
538 modulators of (patho)physiological processes<sup>124–126</sup>. *In vivo* imaging approaches reveal the  
539 time and location of EV-subtype release and the biological fluids in which they are distributed  
540 or accumulate. This “hot spot” mapping could optimize strategies to timely harvest the most  
541 relevant EVs for diagnosis or disease monitoring. High-resolution imaging of injected EVs  
542 purposed for drug delivery can likewise reveal EV pharmacokinetics (half-life, biodistribution,  
543 clearance), fate, and effects on recipient cells in real-time. This supports the development of  
544 engineering and administration protocols for efficient biodistribution and targeting, minimal  
545 clearance, and improved drug delivery efficiency in clinical practice. Monitoring EV dynamics  
546 *in vivo* will also identify drug targets for modulating EV release, uptake and degradation,  
547 influencing pharmacokinetics and EV-intrinsic functions. Thus, *in vivo* imaging approaches  
548 will not only provide crucial insight into fundamental aspects of the EV lifespan but will also  
549 benefit clinical development of EV-based drug delivery systems [Androuin et al., Adv Drug  
550 Del rev under final revision].

551 The future of the field critically depends on a systematic approach comparing the pros and  
552 cons of each EV labeling and imaging strategy, *in vitro* and *in vivo*, to establish their  
553 relevance and good practices. We foresee development of important synergies between  
554 imaging methods and other techniques to investigate EV biology *in vivo*. Imaging is now part  
555 of the toolbox of EV-ologists, who will work with (other) nano-scientists to further elucidate  
556 the biology and therapeutic applications of EVs.

557

558

559

## 560 REFERENCES

- 561 1. Van Niel, G., D’Angelo, G. & Raposo, G. Shedding light on the cell biology of  
562 extracellular vesicles. *Nature Reviews Molecular Cell Biology* vol. 19 213–228  
563 (2018).
- 564 2. Jiang, D. *et al.* Migrasomes provide regional cues for organ morphogenesis  
565 during zebrafish gastrulation. *Nat. Cell Biol.* **21**, 966–977 (2019).
- 566 3. Huang, Y. *et al.* Migrasome formation is mediated by assembly of micron-scale  
567 tetraspanin macrodomains. *Nat. Cell Biol.* **21**, 991–1002 (2019).
- 568 4. Nicolás-Ávila, J. A. *et al.* A Network of Macrophages Supports Mitochondrial  
569 Homeostasis in the Heart. *Cell* **183**, 94-109.e23 (2020).

- 570 5. Melentijevic, I. *et al.* C. elegans neurons jettison protein aggregates and  
571 mitochondria under neurotoxic stress. *Nature* **542**, 367–371 (2017).
- 572 6. Zhang, H. *et al.* Identification of distinct nanoparticles and subsets of  
573 extracellular vesicles by asymmetric flow field-flow fractionation. *Nat. Cell Biol.*  
574 **20**, 332–343 (2018).
- 575 7. Bálint *et al.* Supramolecular attack particles are autonomous killing entities  
576 released from cytotoxic T cells. *Science* **368**, 897–901 (2020).
- 577 8. Marki, A. *et al.* Elongated neutrophil-derived structures are blood-borne  
578 microparticles formed by rolling neutrophils during sepsis. *J. Exp. Med.* **218**,  
579 (2021).
- 580 9. Schubert, D. A brief history of adherons: The discovery of brain exosomes.  
581 *International Journal of Molecular Sciences* vol. 21 1–9 (2020).
- 582 10. Harding, C., Heuser, J. & Stahl, P. Receptor-mediated endocytosis of  
583 transferrin and recycling of the transferrin receptor in rat reticulocytes. *J. Cell*  
584 *Biol.* vol. 97 329–339.
- 585 11. Raposo, G. *et al.* B lymphocytes secrete antigen-presenting vesicles.  
586 *J. Exp. Med.* vol. 183 1161–1172 (1996).
- 587 12. Yáñez-Mó, M. *et al.* Biological properties of extracellular vesicles and their  
588 physiological functions. *J. Extracell. Vesicles* **4**, 27066 (2015).
- 589 13. Budnik, V., Ruiz-Cañada, C. & Wendler, F. Extracellular vesicles round off  
590 communication in the nervous system. *Nat. Rev. Neurosci.* **17**, 160–172  
591 (2016).
- 592 14. Stahl, P. D. & Raposo, G. Extracellular Vesicles: Exosomes and Microvesicles,  
593 Integrators of Homeostasis. *Physiology* **34**, 169–177 (2019).
- 594 15. Boulanger, C. M., Loyer, X., Rautou, P.-E. & Amabile, N. Extracellular vesicles  
595 in coronary artery disease. *Nat. Rev. Cardiol.* **14**, 259–272 (2017).
- 596 16. Jeppesen, D. K. *et al.* Reassessment of Exosome Composition. *Cell* **177**, 428-  
597 445.e18 (2019).
- 598 17. Verweij, F. J. *et al.* Live Tracking of Inter-organ Communication by  
599 Endogenous Exosomes In Vivo. *Dev. Cell* **48**, 573-589.e4 (2019).
- 600 18. van der Vos, K. E. *et al.* Directly visualized glioblastoma-derived extracellular  
601 vesicles transfer RNA to microglia/macrophages in the brain. *Neuro. Oncol.* **18**,  
602 58–69 (2016).
- 603 19. Hyenne, V. *et al.* Studying the Fate of Tumor Extracellular Vesicles at High

- 604 Spatiotemporal Resolution Using the Zebrafish Embryo. *Dev. Cell* **48**, 554-  
605 572.e7 (2019).
- 606 20. Fazeli, G., Trinkwalder, M., Irmisch, L. & Wehman, A. M. C. *C. elegans* midbodies  
607 are released, phagocytosed and undergo LC3-dependent degradation  
608 independent of macroautophagy. *J. Cell Sci.* **129**, 3721–3731 (2016).
- 609 21. Ridder, K. *et al.* Extracellular Vesicle-Mediated Transfer of Genetic Information  
610 between the Hematopoietic System and the Brain in Response to  
611 Inflammation. *PLoS Biol.* **12**, (2014).
- 612 22. Zomer, A. *et al.* In Vivo Imaging Reveals Extracellular Vesicle-Mediated  
613 Phenocopying of Metastatic Behavior. *Cell* **161**, 1046–1057 (2015).
- 614 23. de Jong, O. G. *et al.* A CRISPR-Cas9-based reporter system for single-cell  
615 detection of extracellular vesicle-mediated functional transfer of RNA. *Nat.*  
616 *Commun.* **11**, 1113 (2020).
- 617 24. Gonçalves, M. S. T. Fluorescent Labeling of Biomolecules with Organic  
618 Probes. *Chem. Rev.* **109**, 190–212 (2009).
- 619 25. Pužar Dominkuš, P. *et al.* PKH26 labeling of extracellular vesicles:  
620 Characterization and cellular internalization of contaminating PKH26  
621 nanoparticles. *Biochim. Biophys. Acta. Biomembr.* **1860**, 1350–1361 (2018).
- 622 26. Corso, G. *et al.* Systematic characterization of extracellular vesicles sorting  
623 domains and quantification at the single molecule–single vesicle level by  
624 fluorescence correlation spectroscopy and single particle imaging. *J. Extracell.*  
625 *Vesicles* **8**, (2019).
- 626 27. Collot, M. *et al.* MemBright: A Family of Fluorescent Membrane Probes for  
627 Advanced Cellular Imaging and Neuroscience. *Cell Chem. Biol.* **26**, 600-614.e7  
628 (2019).
- 629 28. Dehghani, M., Gulvin, S. M., Flax, J. & Gaborski, T. R. Exosome labeling by  
630 lipophilic dye PKH26 results in significant increase in vesicle size. *bioRxiv*  
631 (2019) doi:10.1101/532028.
- 632 29. Kuffler, D. P. Long-term survival and sprouting in culture by motoneurons  
633 isolated from the spinal cord of adult frogs. *J. Comp. Neurol.* **302**, 729–38  
634 (1990).
- 635 30. WD, G., AJ, M. & CD, S. An accurate, precise method for general labeling of  
636 extracellular vesicles. *MethodsX* **2**, (2015).
- 637 31. Chuo, S. T.-Y., Chien, J. C.-Y. & Lai, C. P.-K. Imaging extracellular vesicles:

- 638 current and emerging methods. *J. Biomed. Sci.* **25**, 91 (2018).
- 639 32. A, M.-K. *et al.* Labeling Extracellular Vesicles for Nanoscale Flow Cytometry.  
640 *Sci. Rep.* **7**, (2017).
- 641 33. Liao, Z. *et al.* Acetylcholinesterase is not a generic marker of extracellular  
642 vesicles. *J. Extracell. Vesicles* **8**, 1628592 (2019).
- 643 34. Lai, C. P. *et al.* Visualization and tracking of tumour extracellular vesicle  
644 delivery and RNA translation using multiplexed reporters. *Nat. Commun.* **6**,  
645 7029 (2015).
- 646 35. Mittelbrunn, M. *et al.* Unidirectional transfer of microRNA-loaded exosomes  
647 from T cells to antigen-presenting cells. *Nat. Commun.* **2**, 282- (2011).
- 648 36. Mathieu, M., Martin-Jaular, L., Lavieu, G. & Théry, C. Specificities of secretion  
649 and uptake of exosomes and other extracellular vesicles for cell-to-cell  
650 communication. *Nat. Cell Biol.* **21**, 9–17 (2019).
- 651 37. Badr, C. E. & Tannous, B. A. Bioluminescence imaging: Progress and  
652 applications. *Trends in Biotechnology* vol. 29 624–633 (2011).
- 653 38. Takahashi, Y. *et al.* Visualization and in vivo tracking of the exosomes of  
654 murine melanoma B16-BL6 cells in mice after intravenous injection. *J.*  
655 *Biotechnol.* **165**, 77–84 (2013).
- 656 39. Lai, C. P. *et al.* Dynamic Biodistribution of Extracellular Vesicles In Vivo Using  
657 a Multimodal Imaging Reporter. *ACS Nano* **8**, 483 (2014).
- 658 40. AY, W. *et al.* Multiresolution Imaging Using Bioluminescence Resonance  
659 Energy Transfer Identifies Distinct Biodistribution Profiles of Extracellular  
660 Vesicles and Exomeres with Redirected Tropism. *Adv. Sci. (Weinheim, Baden-*  
661 *Wuerttemberg, Ger.* **7**, (2020).
- 662 41. Hoshino, A. *et al.* Tumour exosome integrins determine organotropic  
663 metastasis. *Nature* **527**, 329–35 (2015).
- 664 42. Chen, G. *et al.* Exosomal PD-L1 contributes to immunosuppression and is  
665 associated with anti-PD-1 response. *Nature* **560**, 382–386 (2018).
- 666 43. Ghoroghi, S. *et al.* Ral GTPases promote breast cancer metastasis by  
667 controlling biogenesis and organ targeting of exosomes. *Elife* **10**, (2021).
- 668 44. Zaborowski, M. P. *et al.* Membrane-bound Gaussia luciferase as a tool to track  
669 shedding of membrane proteins from the surface of extracellular vesicles. *Sci.*  
670 *Rep.* **9**, 17387 (2019).
- 671 45. Shinoda, H., Shannon, M. & Nagai, T. Fluorescent Proteins for Investigating

- 672 Biological Events in Acidic Environments. *Int. J. Mol. Sci.* **19**, (2018).
- 673 46. Fan, S. *et al.* Glutamine deprivation alters the origin and function of cancer cell  
674 exosomes. *EMBO J.* **39**, e103009 (2020).
- 675 47. Sung, B. H., Ketova, T., Hoshino, D., Zijlstra, A. & Weaver, A. M. Directional  
676 cell movement through tissues is controlled by exosome secretion. *Nat.*  
677 *Commun.* **6**, 7164 (2015).
- 678 48. Sung, B. H. *et al.* A live cell reporter of exosome secretion and uptake reveals  
679 pathfinding behavior of migrating cells. *Nat. Commun.* **11**, (2020).
- 680 49. Verweij, F. J. *et al.* Quantifying exosome secretion from single cells reveals a  
681 modulatory role for GPCR signaling. *J. Cell Biol.* **217**, 1129–1142 (2018).
- 682 50. Bebelman, M. P. *et al.* Real-time imaging of multivesicular body–plasma  
683 membrane fusion to quantify exosome release from single cells. *Nat. Protoc.*  
684 1–20 (2020) doi:10.1038/s41596-019-0245-4.
- 685 51. Beer, K. B. *et al.* Degron-tagged reporters probe membrane topology and  
686 enable the specific labelling of membrane-wrapped structures. *Nat. Commun.*  
687 **10**, 3490 (2019).
- 688 52. Mustonen, A. M. *et al.* First in vivo detection and characterization of  
689 hyaluronan-coated extracellular vesicles in human synovial fluid. *J. Orthop.*  
690 *Res.* **34**, 1960–1968 (2016).
- 691 53. Choudhuri, K. *et al.* Polarized release of T-cell-receptor-enriched microvesicles  
692 at the immunological synapse. *Nature* **507**, 118–23 (2014).
- 693 54. Saliba, D. G. *et al.* Composition and structure of synaptic ectosomes exporting  
694 antigen receptor linked to functional CD40 ligand from helper T cells. *Elife* **8**,  
695 (2019).
- 696 55. Ambrose, A. R., Hazime, K. S., Worboys, J. D., Niembro-Vivanco, O. & Davis,  
697 D. M. Synaptic secretion from human natural killer cells is diverse and includes  
698 supramolecular attack particles. *Proc. Natl. Acad. Sci. U. S. A.* **117**, 23717–  
699 23720 (2020).
- 700 56. Kanwar, S. S., Dunlay, C. J., Simeone, D. M. & Nagrath, S. Microfluidic device  
701 (ExoChip) for on-chip isolation, quantification and characterization of circulating  
702 exosomes. *Lab Chip* **14**, 1891–900 (2014).
- 703 57. Icha, J., Weber, M., Waters, J. C. & Norden, C. Phototoxicity in live  
704 fluorescence microscopy, and how to avoid it. *BioEssays* vol. 39 (2017).
- 705 58. Spikes, J. D. Photosensitization in Mammalian Cells. in *Photoimmunology* 23–

- 706 49 (Springer US, 1983). doi:10.1007/978-1-4613-3670-9\_2.
- 707 59. Elgamal, S., Colombo, F., Cottini, F., Byrd, J. C. & Cocucci, E. Imaging  
708 intercellular interaction and extracellular vesicle exchange in a co-culture  
709 model of chronic lymphocytic leukemia and stromal cells by lattice light-sheet  
710 fluorescence microscopy. *Methods Enzymol.* **645**, 79–107 (2020).
- 711 60. Buschow, S. I. *et al.* MHC II in dendritic cells is targeted to lysosomes or T cell-  
712 induced exosomes via distinct multivesicular body pathways. *Traffic* **10**, 1528–  
713 42 (2009).
- 714 61. Hurbain, I. *et al.* Microvilli-derived Extracellular Vesicles Govern  
715 Morphogenesis in *Drosophila* wing epithelium. *bioRxiv* 2020.11.01.363697  
716 (2020) doi:10.1101/2020.11.01.363697.
- 717 62. González-Méndez, L. *et al.* Polarized sorting of Patched enables cytoneme-  
718 mediated Hedgehog reception in the *Drosophila* wing disc. *EMBO J.* **39**,  
719 (2020).
- 720 63. Gross, J. C., Chaudhary, V., Bartscherer, K. & Boutros, M. Active Wnt proteins  
721 are secreted on exosomes. *Nat. Cell Biol.* **14**, (2012).
- 722 64. Matusek, T. *et al.* The ESCRT machinery regulates the secretion and long-  
723 range activity of Hedgehog. *Nature* **516**, 99–103 (2014).
- 724 65. Gradilla, A. C. *et al.* Exosomes as Hedgehog carriers in cytoneme-mediated  
725 transport and secretion. *Nat. Commun.* **5**, (2014).
- 726 66. Tassetto, M., Kunitomi, M. & Andino, R. Circulating Immune Cells Mediate a  
727 Systemic RNAi-Based Adaptive Antiviral Response in *Drosophila*. *Cell* **169**,  
728 314-325.e13 (2017).
- 729 67. Härkönen, K. *et al.* CD44s Assembles Hyaluronan Coat on Filopodia and  
730 Extracellular Vesicles and Induces Tumorigenicity of MKN74 Gastric  
731 Carcinoma Cells. *Cells* **8**, 276 (2019).
- 732 68. Abels, E. R. *et al.* Glioblastoma-Associated Microglia Reprogramming Is  
733 Mediated by Functional Transfer of Extracellular miR-21. *Cell Rep.* **28**, 3105-  
734 3119.e7 (2019).
- 735 69. Gupta, D. *et al.* Quantification of extracellular vesicles in vitro and in vivo using  
736 sensitive bioluminescence imaging. *J. Extracell. vesicles* **9**, 1800222 (2020).
- 737 70. Men, Y. *et al.* Exosome reporter mice reveal the involvement of exosomes in  
738 mediating neuron to astroglia communication in the CNS. *Nat. Commun.* **10**,  
739 4136 (2019).

- 740 71. Verweij, F. J., Hyenne, V., Van Niel, G. & Goetz, J. G. Extracellular Vesicles:  
741 Catching the Light in Zebrafish. *Trends in Cell Biology* vol. 29 770–776 (2019).
- 742 72. Wang, J. *et al.* C. elegans ciliated sensory neurons release extracellular  
743 vesicles that function in animal communication. *Curr. Biol.* **24**, 519–25 (2014).
- 744 73. Wehman, A. M., Poggioli, C., Schweinsberg, P., Grant, B. D. & Nance, J. The  
745 P4-ATPase TAT-5 inhibits the budding of extracellular vesicles in C. elegans  
746 embryos. *Curr. Biol.* **21**, 1951–1959 (2011).
- 747 74. Hyenne, V. *et al.* hRAL-1 controls multivesicular body biogenesis and exosome  
748 secretion. *J. Cell Biol.* **211**, 27–37 (2015).
- 749 75. Baumeister, R. & Ge, L. The worm in us - Caenorhabditis elegans as a model  
750 of human disease. *Trends Biotechnol.* **20**, 147–8 (2002).
- 751 76. Howe, K. *et al.* The zebrafish reference genome sequence and its relationship  
752 to the human genome. *Nature* **496**, 498–503 (2013).
- 753 77. Fortini, M. E., Skupski, M. P., Boguski, M. S. & Hariharan, I. K. A survey of  
754 human disease gene counterparts in the Drosophila genome. *J. Cell Biol.* **150**,  
755 F23-30 (2000).
- 756 78. Santoriello, C. & Zon, L. I. Hooked! Modeling human disease in zebrafish. *J.*  
757 *Clin. Invest.* **122**, 2337–43 (2012).
- 758 79. Caygill, E. E. & Brand, A. H. The GAL4 System: A Versatile System for the  
759 Manipulation and Analysis of Gene Expression. in 33–52 (Humana Press, New  
760 York, NY, 2016). doi:10.1007/978-1-4939-6371-3\_2.
- 761 80. Port, F. *et al.* A large-scale resource for tissue-specific CRISPR mutagenesis in  
762 Drosophila. *Elife* **9**, (2020).
- 763 81. Albadri, S., De Santis, F., Di Donato, V. & Del Bene, F. CRISPR/Cas9-  
764 mediated knockin and knockout in Zebrafish. in *Research and Perspectives in*  
765 *Neurosciences* 41–49 (2017). doi:10.1007/978-3-319-60192-2\_4.
- 766 82. Muntasell, A., Berger, A. C. & Roche, P. A. T cell-induced secretion of MHC  
767 class II-peptide complexes on B cell exosomes. *EMBO J.* vol. 26 4263–4272  
768 (2007).
- 769 83. Lachenal, G. *et al.* Release of exosomes from differentiated neurons and its  
770 regulation by synaptic glutamatergic activity. *Mol. Cell. Neurosci.* **46**, 409–418  
771 (2011).
- 772 84. Li, J. *et al.* Serum-free culture alters the quantity and protein composition of  
773 neuroblastoma-derived extracellular vesicles. *J. Extracell. vesicles* **4**, 26883

- 774 (2015).
- 775 85. Rocha, S. *et al.* 3D Cellular Architecture Affects MicroRNA and Protein Cargo  
776 of Extracellular Vesicles. *Adv. Sci.* **6**, 1800948 (2019).
- 777 86. Thippabhotla, S., Zhong, C. & He, M. 3D cell culture stimulates the secretion of  
778 in vivo like extracellular vesicles. *Sci. Rep.* **9**, 13012 (2019).
- 779 87. Cao, J. *et al.* Three-dimensional culture of MSCs produces exosomes with  
780 improved yield and enhanced therapeutic efficacy for cisplatin-induced acute  
781 kidney injury. *Stem Cell Res. Ther.* **11**, 206 (2020).
- 782 88. Kim, M., Yun, H.-W., Park, D. Y., Choi, B. H. & Min, B.-H. Three-Dimensional  
783 Spheroid Culture Increases Exosome Secretion from Mesenchymal Stem  
784 Cells. *Tissue Eng. Regen. Med.* **15**, 427–436 (2018).
- 785 89. Lehrich, B. M., Liang, Y. & Fiandaca, M. S. Foetal bovine serum influence on in  
786 vitro extracellular vesicle analyses. *J. Extracell. Vesicles* **10**, (2021).
- 787 90. Chen, L., Ma, L. & Yu, L. WGA is a probe for migrasomes. *Cell Discovery* vol. 5  
788 13 (2019).
- 789 91. Ma, L. *et al.* Discovery of the migrasome, an organelle mediating release of  
790 cytoplasmic contents during cell migration. *Cell Res.* **25**, 24–38 (2015).
- 791 92. Addi, C. *et al.* The Flemmingsome reveals an ESCRT-to-membrane coupling  
792 via ALIX/syntenin/syndecan-4 required for completion of cytokinesis. *Nat.*  
793 *Commun.* **11**, 1941 (2020).
- 794 93. Miesenbock, G., De Angelis, D. A. & Rothman, J. E. Visualizing secretion and  
795 synaptic transmission with pH- sensitive green fluorescent proteins. *Nature*  
796 **394**, 192–195 (1998).
- 797 94. Cashikar, A. G. & Hanson, P. I. A cell-based assay for CD63-containing  
798 extracellular vesicles. *PLoS One* **14**, e0220007 (2019).
- 799 95. Wegner, C. S. *et al.* Ultrastructural characterization of giant endosomes  
800 induced by GTPase-deficient Rab5. *Histochem. Cell Biol.* **133**, 41–55 (2010).
- 801 96. Mathieu, M. *et al.* Specificities of exosome versus small ectosome secretion  
802 revealed by live intracellular tracking and synchronized extracellular vesicle  
803 release of CD9 and CD63. *bioRxiv* 2020.10.27.323766 (2020)  
804 doi:10.1101/2020.10.27.323766.
- 805 97. Lenzini, S., Bargi, R., Chung, G. & Shin, J. W. Matrix mechanics and water  
806 permeation regulate extracellular vesicle transport. *Nat. Nanotechnol.* **15**, 217–  
807 223 (2020).



- 808 98. Mu, W., Rana, S. & Zöller, M. Host Matrix Modulation by Tumor Exosomes  
809 Promotes Motility and Invasiveness. *Neoplasia* **15**, 875-IN4 (2013).
- 810 99. Wiklander, O. P. B. *et al.* Extracellular vesicle in vivo biodistribution is  
811 determined by cell source, route of administration and targeting. *J. Extracell.*  
812 *Vesicles* **4**, (2015).
- 813 100. Ridder, K. *et al.* Extracellular vesicle-mediated transfer of functional RNA in the  
814 tumor microenvironment. *Oncoimmunology* **4**, e1008371 (2015).
- 815 101. Riau, A. K., Ong, H. S., Yam, G. H. F. & Mehta, J. S. Sustained Delivery  
816 System for Stem Cell-Derived Exosomes. *Front. Pharmacol.* **10**, 1368 (2019).
- 817 102. Rilla, K. *et al.* Extracellular vesicles are integral and functional components of  
818 the extracellular matrix. *Matrix Biology* vols 75–76 201–219 (2019).
- 819 103. Pastuzyn, E. D. *et al.* The Neuronal Gene Arc Encodes a Repurposed  
820 Retrotransposon Gag Protein that Mediates Intercellular RNA Transfer. *Cell*  
821 **172**, 275-288.e18 (2018).
- 822 104. Ashley, J. *et al.* Retrovirus-like Gag Protein Arc1 Binds RNA and Traffics  
823 across Synaptic Boutons. *Cell* **172**, 262-274.e11 (2018).
- 824 105. Edgar, J. R., Manna, P. T., Nishimura, S., Banting, G. & Robinson, M. S.  
825 Tetherin is an exosomal tether. *Elife* **5**, (2016).
- 826 106. Morad, G. *et al.* Tumor-Derived Extracellular Vesicles Breach the Intact Blood-  
827 Brain Barrier via Transcytosis. *ACS Nano* **13**, 13853 (2019).
- 828 107. Alvarez-Erviti, L. *et al.* Delivery of siRNA to the mouse brain by systemic  
829 injection of targeted exosomes. *Nat. Biotechnol.* **29**, 341–345 (2011).
- 830 108. Denzer, K. *et al.* Follicular dendritic cells carry MHC class II-expressing  
831 microvesicles at their surface. *J. Immunol.* **165**, 1259–65 (2000).
- 832 109. Gao, L. *et al.* Tumor-derived exosomes antagonize innate antiviral immunity.  
833 *Nat. Immunol.* **19**, 233–245 (2018).
- 834 110. Vilcaes, A. A., Chanaday, N. L. & Kavalali, E. T. Interneuronal exchange and  
835 functional integration of synaptobrevin via extracellular vesicles. *Neuron* **109**,  
836 971-983.e5 (2021).
- 837 111. Ko, S. Y. *et al.* Cancer-derived small extracellular vesicles promote  
838 angiogenesis by heparin-bound, bevacizumab-insensitive VEGF, independent  
839 of vesicle uptake. *Commun. Biol.* **2**, (2019).
- 840 112. Neumann, C. J. & Cohen, S. M. Long-range action of Wingless organizes the  
841 dorsal-ventral axis of the *Drosophila* wing. *Development* **124**, 871–80 (1997).

- 842 113. Tkach, M. *et al.* Qualitative differences in T-cell activation by dendritic cell-  
843 derived extracellular vesicle subtypes. *EMBO J.* **36**, 3012–3028 (2017).
- 844 114. Heusermann, W. *et al.* Exosomes surf on filopodia to enter cells at endocytic  
845 hot spots and shuttle within endosomes to scan the ER. *J. Cell Biol.* **213**, Final  
846 revised manuscript submitted (2016).
- 847 115. Arasu, U. T., Härkönen, K., Koistinen, A. & Rilla, K. Correlative light and  
848 electron microscopy is a powerful tool to study interactions of extracellular  
849 vesicles with recipient cells. *Exp. Cell Res.* **376**, 149–158 (2019).
- 850 116. Thomou, T. *et al.* Adipose-derived circulating miRNAs regulate gene  
851 expression in other tissues. *Nature* **542**, 450–455 (2017).
- 852 117. Sterzenbach, U. *et al.* Engineered Exosomes as Vehicles for Biologically Active  
853 Proteins. *Mol. Ther.* **25**, 1269–1278 (2017).
- 854 118. Kur, I.-M. *et al.* Neuronal activity triggers uptake of hematopoietic extracellular  
855 vesicles in vivo. *PLoS Biol.* **18**, e3000643 (2020).
- 856 119. Frühbeis, C. *et al.* Neurotransmitter-triggered transfer of exosomes mediates  
857 oligodendrocyte-neuron communication. *PLoS Biol.* **11**, e1001604 (2013).
- 858 120. Khmelinskii, A. *et al.* Incomplete proteasomal degradation of green fluorescent  
859 proteins in the context of tandem fluorescent protein timers. *Mol. Biol. Cell* **27**,  
860 360–70 (2016).
- 861 121. Joshi, B. S., De Beer, M. A., Giepmans, B. N. G. & Zuhorn, I. S. Endocytosis of  
862 Extracellular Vesicles and Release of Their Cargo from Endosomes. *ACS*  
863 *Nano* **14**, 32 (2020).
- 864 122. Cao, H. *et al.* In Vivo Real-Time Imaging of Extracellular Vesicles in Liver  
865 Regeneration via Aggregation-Induced Emission Luminogens. *ACS Nano* **13**,  
866 3522–3533 (2019).
- 867 123. Webber, J. P. *et al.* Differentiation of tumour-promoting stromal myfibroblasts  
868 by cancer exosomes. *Oncogene* **34**, 290–302 (2015).
- 869 124. Lener, T. *et al.* Applying extracellular vesicles based therapeutics in clinical  
870 trials - an ISEV position paper. *J. Extracell. vesicles* **4**, 30087 (2015).
- 871 125. Fais, S. *et al.* Evidence-Based Clinical Use of Nanoscale Extracellular Vesicles  
872 in Nanomedicine. *ACS Nano* **10**, 3886–99 (2016).
- 873 126. Kalluri, R. & LeBleu, V. S. The biology, function, and biomedical applications of  
874 exosomes. *Science* **367**, (2020).
- 875 127. Liégeois, S., Benedetto, A., Garnier, J.-M., Schwab, Y. & Labouesse, M. The

- 876 V0-ATPase mediates apical secretion of exosomes containing Hedgehog-  
877 related proteins in *Caenorhabditis elegans*. *J. Cell Biol.* **173**, 949–961 (2006).
- 878 128. Koles, K. *et al.* Mechanism of evenness interrupted (Evi)-exosome release at  
879 synaptic boutons. *J. Biol. Chem.* **287**, 16820–34 (2012).
- 880 129. Corrigan, L. *et al.* BMP-regulated exosomes from *Drosophila* male reproductive  
881 glands reprogram female behavior. *J. Cell Biol.* **206**, 671–88 (2014).
- 882 130. Wolf, P. The Nature and Significance of Platelet Products in Human Plasma.  
883 *Br. J. Haematol.* **13**, 269–288 (1967).
- 884 131. Nunez, E. A., Wallis, J. & Gershon, M. D. Secretory processes in follicular cells  
885 of the bat thyroid. III. The occurrence of extracellular vesicles and colloid  
886 droplets during arousal from hibernation. *Am. J. Anat.* **141**, 179–201 (1974).
- 887 132. Trams, E. G., Lauter, C. J., Norman Salem, J. & Heine, U. Exfoliation of  
888 membrane ecto-enzymes in the form of micro-vesicles. *Biochim. Biophys. Acta*  
889 *- Biomembr.* **645**, 63–70 (1981).
- 890 133. Johnstone, R. M., Bianchini, A. & Teng, K. Reticulocyte maturation and  
891 exosome release: transferrin receptor containing exosomes shows multiple  
892 plasma membrane functions. *Blood* **74**, 1844–51 (1989).
- 893 134. Heijnen, H. F., Schiel, A. E., Fijnheer, R., Geuze, H. J. & Sixma, J. J. Activated  
894 platelets release two types of membrane vesicles: microvesicles by surface  
895 shedding and exosomes derived from exocytosis of multivesicular bodies and  
896 alpha-granules. *Blood* vol. 94 3791–3799.
- 897 135. Yang, T. *et al.* Exosome Delivered Anticancer Drugs Across the Blood-Brain  
898 Barrier for Brain Cancer Therapy in *Danio Rerio*. *Pharm. Res.* **32**, 2003–2014  
899 (2015).

900

901 **Glossary:**

902 *Page 4:*

903 **Glycan extended trees**

904 protein modification consisting of attached polymerized glycans possessing structural and/or  
905 modulatory function (e.g. ligand binding)

906

907 *Page 5:*

908 **Lipid membrane dye**

909 lipophilic fluorescent dye that integrates in lipid membranes

910

911 *Page 6:*

912 **EV subtype**

913 EV with specific (sub)cellular origin, size, and/or composition (**Table 1**)  
914  
915 **Tetraspanin**  
916 Family of membrane proteins with 4 transmembrane domains enriched in EVs.  
917  
918 **Inner leaflet**  
919 cytosol- or EV lumen-facing layer of a lipid bilayer  
920  
921 **Fluorescent complementation:** a technology used to validate protein interactions through  
922 the association of complementary fluorescent protein fragments attached to components of  
923 the same macromolecular complex.  
924  
925 **Steric hindrance**  
926 here: spatial extent of an exogenous label preventing native interaction(s) of the labelled  
927 protein  
928  
929 **EV cargo**  
930 any molecule (lipid, protein, metabolite, genetic material) shuttled within or on EVs  
931  
932 *Page 7:*  
933 **CLEM**  
934 Imaging technique to correlate (live) light-microscopy with ultrastructural information  
935 obtained on the same sample after fixation  
936  
937 **Diffraction-limit**  
938 Theoretical limit of optical microscopes to distinguish objects separated by a lateral distance  
939 less than half the wavelength used  
940  
941 *Page 8:*  
942 **Photo-bleaching**  
943 Photon-induced alteration of a fluorophore causing it to permanently lose its ability to  
944 fluoresce  
945  
946 **Photo-toxicity**  
947 Photon-induced damage to cellular macromolecules that impairs sample physiology  
948  
949 **Intraluminal Vesicles**  
950 Vesicles formed inside endosomes and precursors of canonical exosomes (*Table 1*)  
951  
952 *Page 9:*  
953 **3D microenvironment**  
954 local environment surrounding a cell, consisting of ECM, soluble factors and other cells  
955  
956 *Page 10:*  
957 **Gene traps**  
958 Here: insertion of fluorescent tag such that the labelled protein is expressed under its  
959 endogenous promoter

960

961 *Page 11:*

962 **Lectins**

963 Saccharide binding proteins

964

965 **Midbody remnants**

966 Condensed membrane structure derived from the intercellular bridge that is left over after  
967 cell division

968

969 *Page 15:*

970 **V-ATPase**

971 Transmembrane proton pump functioning to acidify intracellular compartments

972

973 **Back-fusion**

974 Process where ILVs or internalized EVs fuse with the late-endosomal limiting membrane,  
975 exposing their lumen to the cytosol and delivering their luminal content to the cytoplasm of  
976 recipient cells.

977  
978  
979  
980  
981  
982  
983  
984  
985  
986  
987  
988  
989  
990  
991  
992  
993  
994  
995  
996  
997  
998  
999  
1000  
1001  
1002  
1003  
1004  
1005  
1006  
1007  
1008  
1009  
1010  
1011  
1012  
1013

**Table legends:**

1) Extracellular vesicles and Particles

Extracellular vesicles (EVs) comprise a heterogeneous population of membrane vesicles. Their sizes vary between <50 nm and >5 µm. They can originate from the plasma membrane, the endosomal or autophagic pathway. MVB: multivesicular body; ND: not determined.

2) Tagging strategies of EVs

Different labeling strategies are suitable for visualizing EV (subtype) biogenesis, secretion, transfer, biodistribution, uptake and functional (cargo) transfer, as well as to image at sub-cellular or body wide resolution using live- or fixed imaging. (-) unsuitable; (-/+) low suitability; (+) suitable; (++) highly suitable. CM, confocal microscopy; SDM, spinning-disk microscopy; BFM, bright field microscopy; SPECT, single photon emission computed tomography; PET, positron emission tomography; (i)EM, (immuno-)electron microscopy; TIRFM, total internal reflection fluorescence microscopy; BLIM, bioluminescence imaging microscopy

3) Microscopy methods

**Top:** Schematic of the resolution of different microscopic approaches to resolve EVs at increasing resolution. **Bottom:** Characteristics of imaging methods used to visualize EVs. SIM, structured illumination microscopy; STED, stimulated emission depletion; PALM, photo activated localization microscopy; STORM, stochastic optical reconstruction microscopy; LLSM, lattice light-sheet microscopy; (T)EM, (transmission) electron microscopy; CLEM, correlative light electron microscopy; epi, epifluorescence; TIRF, total internal reflection fluorescence; FP, fluorescent proteins; sec, seconds; min, minutes; FTT, fast Fourier transform; PSF, point spread function.

4) EV imaging model systems

The suitability and relevance of different model systems for EV imaging to visualize disparate aspects of EV biology at different scales. (-) unsuitable; (-/+) low suitability; (+) suitable; (++) highly suitable.

**Refs in table**

CAM<sup>47,67</sup>  
*C. elegans*<sup>72-74,127</sup>  
*D. melanogaster*<sup>63-65,128,129</sup>

1014 *D. rerio*<sup>2,17,19</sup>

1015 *M. musculus*, *R. norvegicus*<sup>21,22,34,118</sup>

1016

1017 **BOX LEGENDS**

1018 **Box 1:** Timeline of EV imaging milestones.

1019 Timeline references:

1020

1021 Wolf et al., 1967<sup>130</sup>; Nunez et al 1974<sup>131</sup>; Trams et al 1981<sup>132</sup>; Harding et al 1983<sup>10</sup>;

1022 Johnstone et al 1989<sup>133</sup>; Heijnen et al 1999<sup>134</sup>; Liegeois et al 2006<sup>127</sup>; Wehman et al 2011

1023 <sup>73</sup>; Koles et al 2012<sup>128</sup>; Gross et al 2012<sup>63</sup>; Takahashi et al 2013<sup>38</sup>; Yang et al 2015<sup>135</sup>;

1024 Sung et al 2015<sup>47</sup>; Zomer et al 2015<sup>22</sup>; Lai et al 2015<sup>34</sup>; Verweij et al 2019<sup>17</sup>; Hyenne et al

1025 2019<sup>19</sup>; Jiang et al 2019<sup>2</sup>

1026

1027

1028 **FIGURE LEGENDS**

1029 **Figure 1 - Tagging strategies to image EV production:**

1030 **A.** Extracellular vesicles (EVs) are diverse double-leaflet membrane-enclosed structures

1031 generated from the plasma membrane (microvesicles, apoptotic bodies, oncosomes,

1032 exophers, enveloped viruses, and migrasomes), from endosomal compartments (exosomes

1033 and enveloped retroviruses), and from autophagic compartments (secretory

1034 autophagosomes). The origin of exomeres is still uncertain. **B-E.** Tagging strategies to image

1035 EVs. **B.** Cytoplasmic labeling facilitates pan-EV tagging by labeling the cell cytosol and the

1036 lumen of any EVs. Right: Large EVs released from MDA-MB-231 cells expressing Dendra2 in

1037 mice mammary glands<sup>22</sup>. **C.** Membrane labelling tags multiple EV subtypes. Right: Confocal

1038 microscopy of live PalmGFP-expressing 293T cells releasing EVs<sup>34</sup>. **D.** Expressing tagged cargo

1039 proteins allows the tracking of EV subtypes. Right: Live-imaging of a burst of CD63-pHluorin

1040 fluorescence at the HeLa cell surface (1,2) overlaid using CLEM (3) to observe an MVB

1041 fusing with the plasma membrane to release exosomes (4)<sup>49</sup>. **E.** Expression of degron-tagged

1042 fluorescent proteins allows EV tagging while cytosolic fluorescence in the source cell is

1043 degraded. Right: PH::CTPD-labeled EVs released from the unlabeled plasma membrane in *C.*

1044 *elegans*<sup>51</sup>. **F.** Targeting of EV surface proteins by antibodies. Right: Optical-EM correlation of

1045 *M. musculus* T cell (1) that released EVs (red)<sup>53</sup>. Single EV imaging (2) by dSTORM analysis of

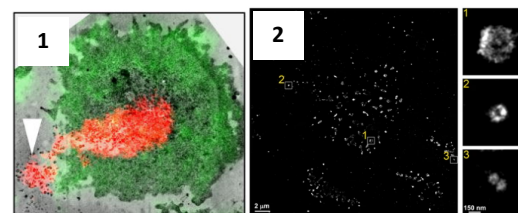
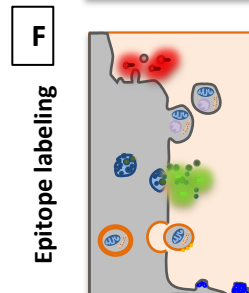
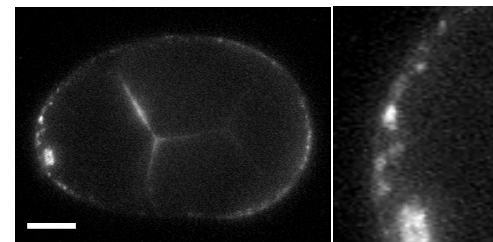
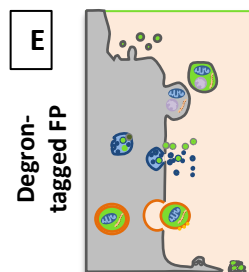
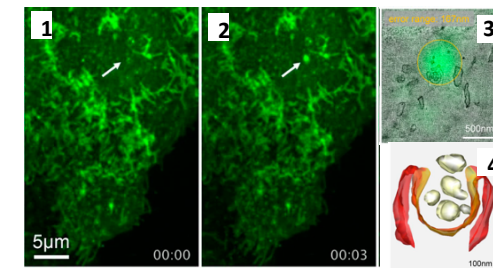
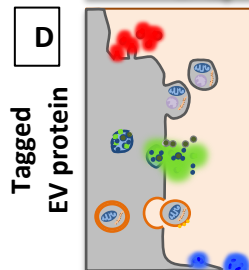
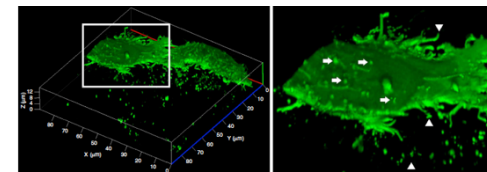
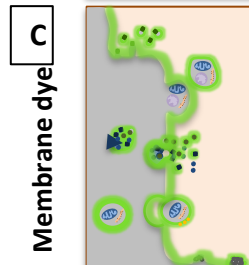
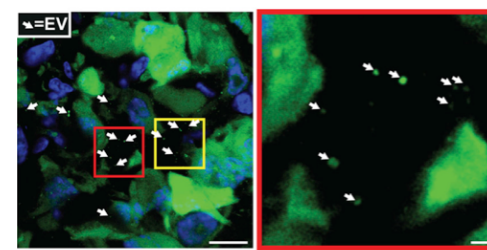
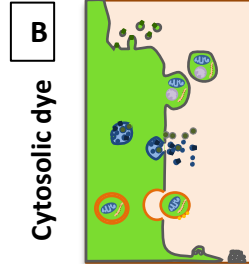
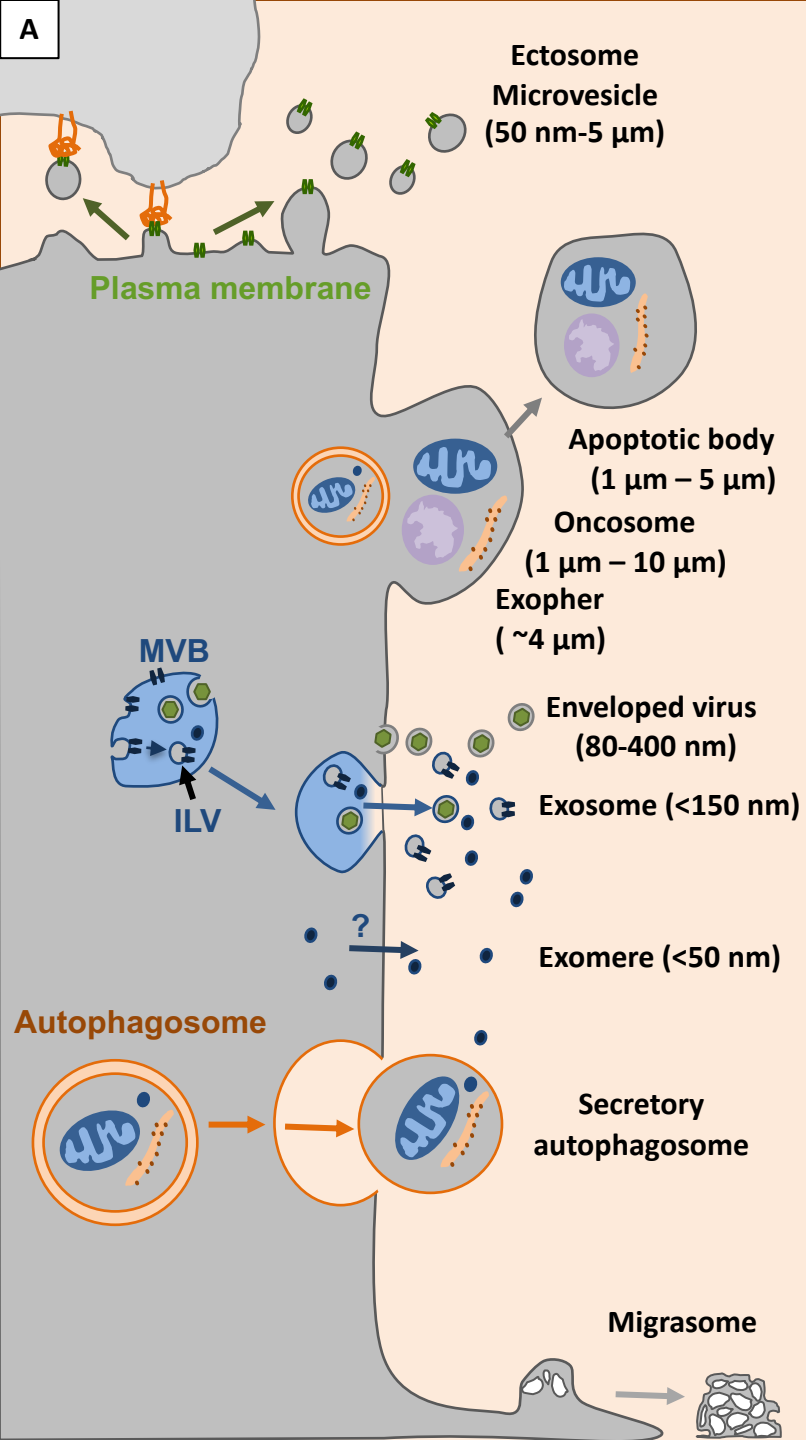
1046 antibody staining<sup>54</sup>.

1047 **Figure 2 – Imaging EV propagation *in vivo***

1048 **A.** EV biodistribution can be mapped in the complex architecture of an organism after  
1049 injection of labeled exogenous EVs or tagging endogenous EVs *in situ*. The *in vivo* fates of EVs  
1050 (white boxes) are illustrated. **B-E:** Imaging using injected or endogenous EVs in live animals.  
1051 **(B)** EV accumulation tracked at the organ scale using CD63-ThermoLuciferase in mice<sup>69</sup>. **(C)**  
1052 EVs interacting with endothelial cells (top) or macrophages (middle) tracked live in  
1053 transparent zebrafish *D. rerio*. EV circulation in comparison to red blood cells (RBCs)  
1054 (bottom)<sup>19</sup>. **(D)** Endogenous EV clearance by scavenger cells in *D. rerio* (top). Immuno-  
1055 electron microscopy confirms the vesicular nature of the CD63-pHluorin signal *in situ*  
1056 (bottom right)<sup>17</sup>. **E-F:** Fluorescently-tagged EV cargo proteins track released EVs in *C. elegans*  
1057 **(E)**<sup>72</sup> and *D. melanogaster* **(F)**<sup>129</sup>.



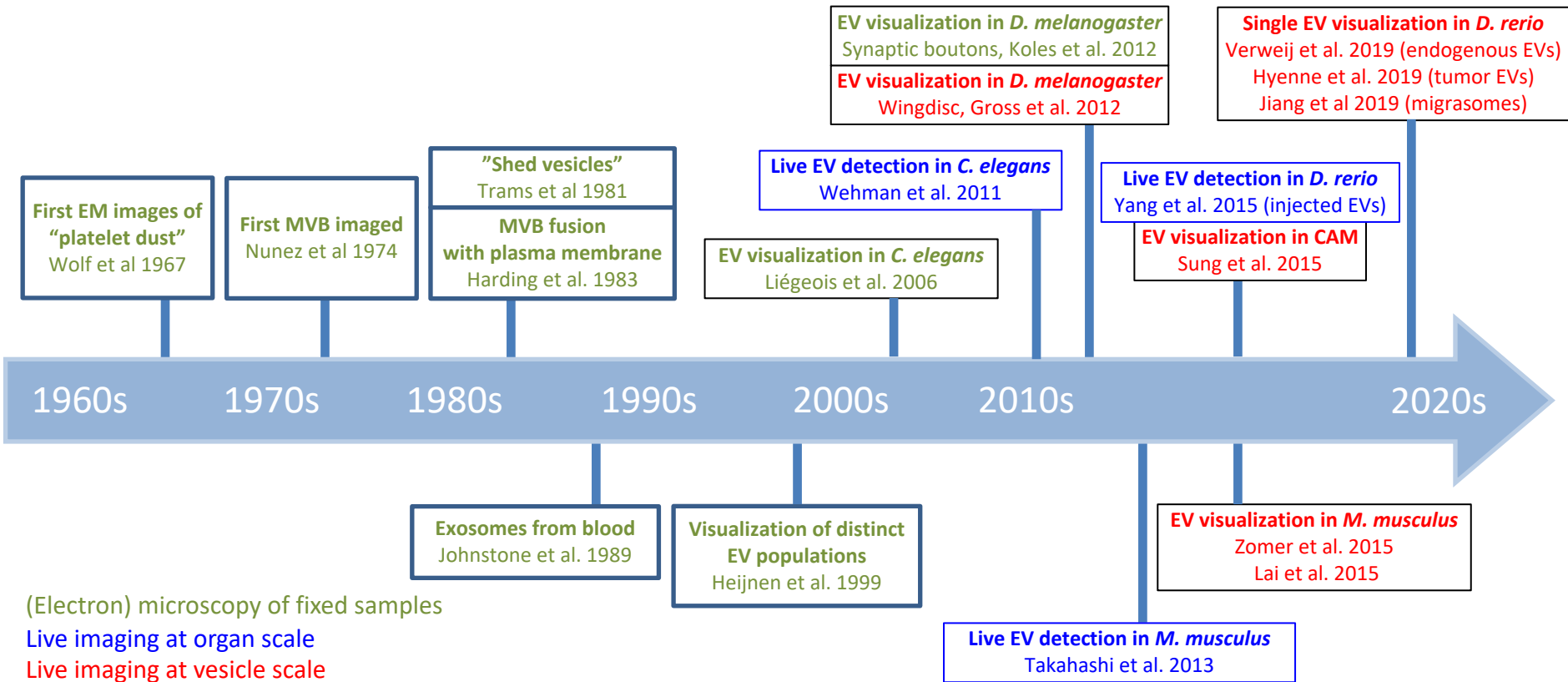
1058 **Figure 3 – Tagging strategies to image EV interaction, uptake and fate**  
1059 **A.** Different tagging strategies (blue box) reveal distinct aspects of EV-cell interactions. **B-F:**  
1060 Imaging strategies to track the fate and functions of EVs. **B.** Correlative light and scanning  
1061 electron microscopy shows GFP-HAS3-labeled EVs interacting with the plasma membrane of  
1062 receiving cells<sup>115</sup>. **C.** Top: Tracking uptake of endogenous CD63-pHluorin-labeled EVs in the  
1063 *D. rerio* vasculature<sup>17</sup>. Bottom: Tracking double-labeled pHluorin-CD63-mScarlet EVs in- and  
1064 outside HT1080 cells<sup>48</sup>. **D.** *Ex-vivo* mapping of EV mRNA using a Cre recombinase strategy in  
1065 the mouse brain<sup>118</sup>. **E.** Correlative light and electron microscopy shows Membright Cy3 lipid  
1066 dye-labeled EVs accumulating in endolysosomes in *D. rerio* vascular cells<sup>19</sup>.



## Extracellular Vesicles and Particles

name	size	acronyms/other names	origin	features
exosomes	50 nm - 150 nm	tolerosomes, dendrosomes, prostasomes, prominosomes	MVBs, late- or recycling endosomes, amphisomes	lipid bilayer; contains: proteins, genetic material, metabolites
microvesicles	50 nm - 5 µm	MVs; ectosomes, microparticles, synaptosomes, myelosome	plasma membrane	lipid bilayer; contains: proteins, genetic material, metabolites
apoptotic bodies	1 µm - 5 µm	apoptotic blebs	plasma membrane	lipid bilayer; contains: proteins, cytosolic components, organelles, nuclear fragments
oncosomes	100 nm - 400 nm		plasma membrane	lipid bilayer; contains: (onco)proteins, genetic material, (onco)metabolites
large oncosomes	1 µm - >10 µm	LO	plasma membrane	lipid bilayer; contains peculiar cancer cell metabolism related enzymes
enveloped viruses	80 nm - 400 nm		endosomes, plasma membrane	lipid bilayer, virion, viral proteins, viral genetic material
exomeres	<50 nm		ND	might lack a lipid bilayer; contains proteins such as argonaute and APP, lipids and nucleic acids
exophers	4 µm		plasma membrane	lipid bilayer; contains metabolic waste, protein aggregates, organelles
secretory autophagosomes	0.5 µm - 2 µm	mitovesicles ?	autophagic pathway	lipid bilayer; contains cytoplasmic contents, excess/damaged proteins, organelles, microorganisms
migrasomes	50 nm - 3 µm		plasma membrane-derived retraction fibers	lipid bilayer; cytoplasmic content
supramolecular attack particles	120 nm	SMAPs	ND, cytotoxic granules	no lipid bilayer; cytotoxic core surrounded by thrombospondin-1 shell
elongated particles	1.9 – 112 µm	shear-derived particles, SDP	plasma membrane	lipid bilayer; shear-derived particle, observed in rolling neutrophils

# Box 1 Timeline of selected EV imaging milestones



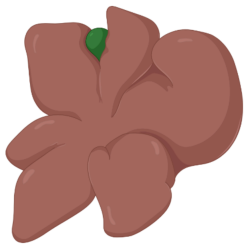
Suitability for visualizing:	Biogenesis	Secretion	Transfer	Biodistribution	Uptake	Functional transfer	Sub-cellular Resolution	Body-wide Resolution	Microscopy techniques	Live or fixed
<b>Lipid dyes</b>										
PKH, MemBright, Dil, DiO, DiR	-	-/+	+	+	+	-	+	-/+	CM, SDM, BFM	live, fixed
<b>Radio-/metabolic labels</b>										
radioisotopes (i.e. 99mTc)	-	-	-	++	-	-	-	++	SPECT, PET	live
Metabolic labelling (e.g. Glycan)	-	-	-	++	+	-	-/+	++	BFM, ...	live
<b>Genetic labelling strategies</b>										
Protein fused to FP (e.g. TSPAN-XFP)	+	++	+	+	+	-	+		iEM, CM, SDM, TIRFM, BFM	live, fixed
degron tagging	-	+	+	+	+	-	+		CM, SDM, BFM	live, fixed
Cre/LoxP	-	-	-	-/+	-/+	++	+		CM, SDM, BFM	live, fixed
Apex	+	-	-	-	+	+	+		EM	fixed
nanoluciferase	-	+	-	+	+	-	+	++	BLIM, iEM	live, fixed

Standard fluorescence microscopy

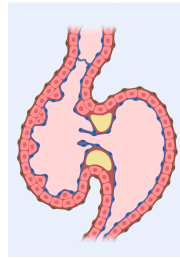
SIM/STED/Cryo-soft X-ray/PALM/STORM/LLSM

EM/CLEM

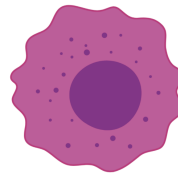
10<sup>-1</sup> m      10<sup>-2</sup> m      10<sup>-3</sup> m      10<sup>-4</sup> m      10<sup>-5</sup> m      10<sup>-6</sup> m      10<sup>-7</sup> m      10<sup>-8</sup> m      10<sup>-9</sup> m  
 10 cm      1 cm      1 mm      100 μm      10 μm      1 μm      100 nm      10 nm      1 nm



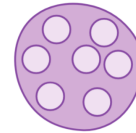
Mouse tissue



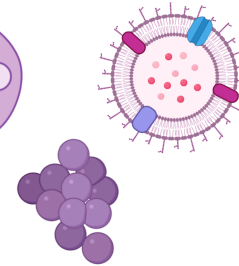
Lower organism tissue



Cell



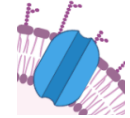
Organelles (MVB)



EV cluster



Single EV



Protein Membrane bilayer

Modalities	Resolution (XY)	Resolution (Z)	Illumination	Probes	Acquisition time	Post-acquisition processing	Live or fixed	Promiscuous
Standard Fluorescence microscopy	250 nm	500 nm	Epi, confocal, TIRF	Conventional fluorescent probes	sec		both	
SIM, airyscan	80-150 nm	250-350 nm	Widefield (epi and TIRF)	Conventional fluorescent probes	sec	Yes, FTT	both	
STED	30-80 nm	150 nm	Laser scanning	Limited selection of probes (match depletion laser)	sec	no	both, optimal for fixed	
Cryo-soft X-ray tomography	25-40 nm	30 nm	Widefield	none		no	fixed (near-native state vitrification)	
PALM	20 nm	50 nm	Widefield (epi and TIRF)	Photo-activatable FPs	min	Yes (PSF mapping)	both	
STORM	20 nm	50 nm	Widefield (epi and TIRF)	Photoswitchable dyes	min	Yes PSF mapping	both	
LLSM	100-200 nm	400 nm	multi-Bessel beam plane illumination	Conventional fluorescent probes	Sec-min-hours	Not necessary, but often tracking dynamic processes	both, optimal for live	
(T)EM /CLEM	<1 nm	70 nm*	electron beam	Contrast reagent, immunochemistry	sec	Yes	fixed	*resolution corresponding to the thickness of the section.
(T)EM /CLEM	<1 nm /150 nm*	5 nm**	electron beam	Contrast reagent, nanodots, and FPs	min	Yes (aligning)	fixed	*resolution gap between light- and electron microscopy data resp **Tomography from double tilted 250 nm sections

# Figure 2 – Imaging EV distribution *in vivo*

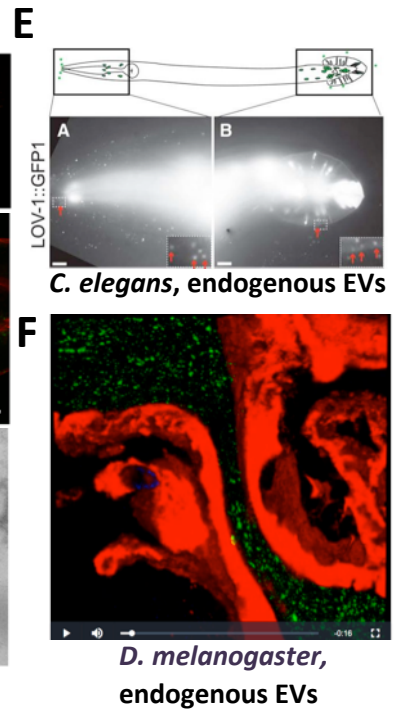
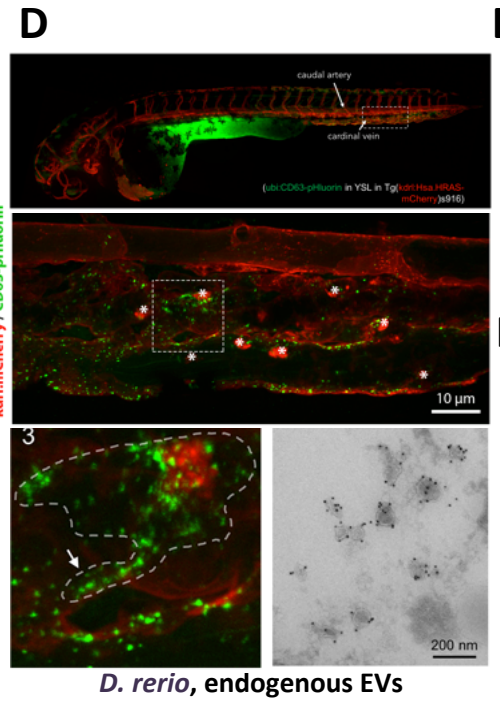
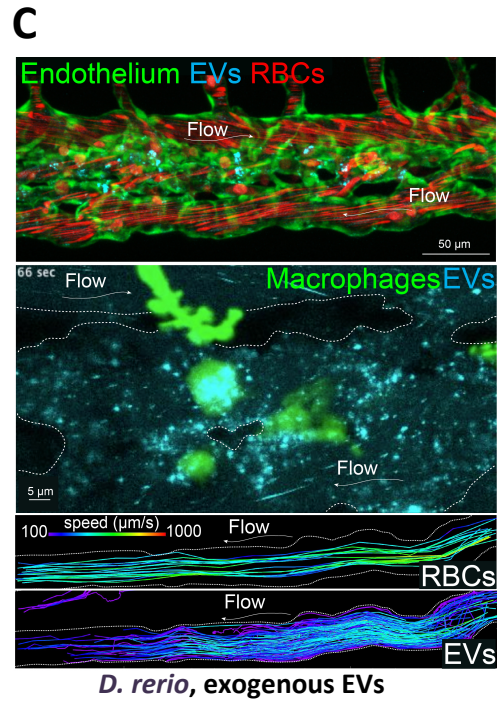
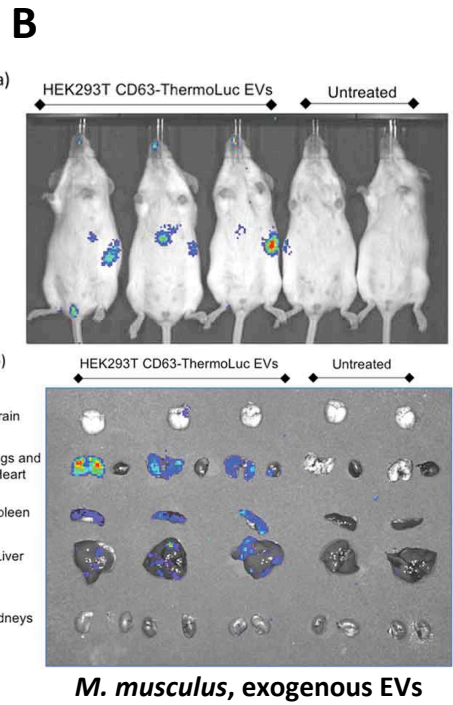
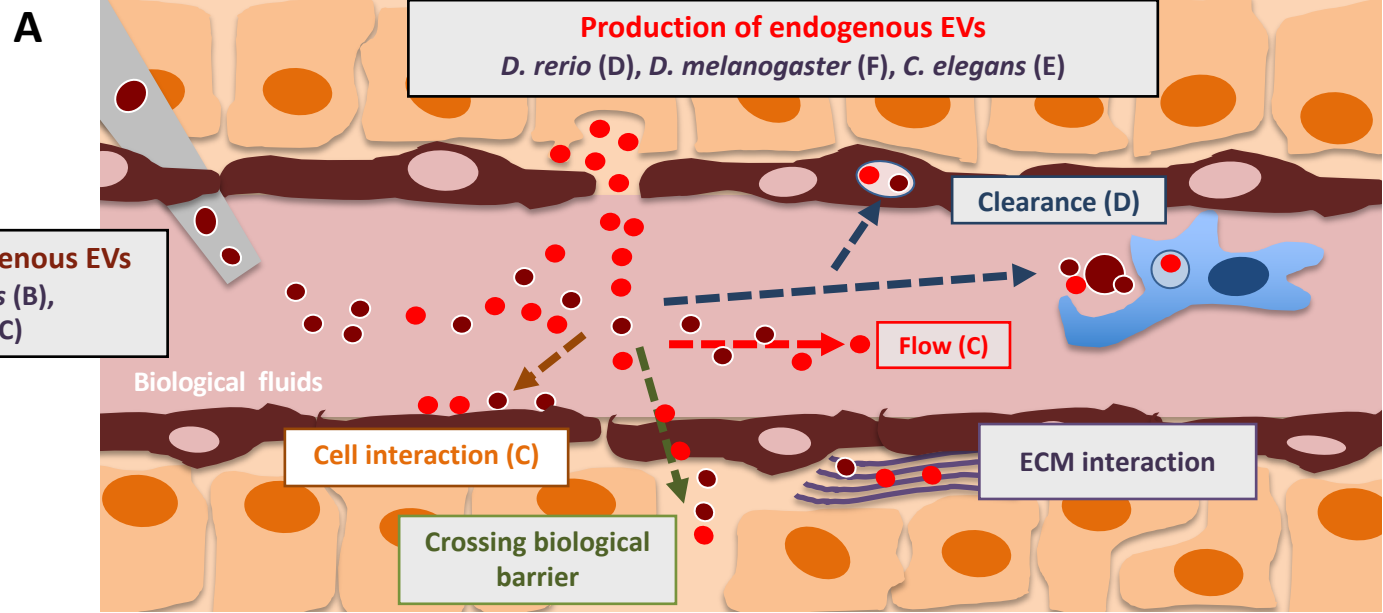
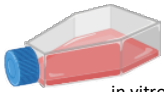
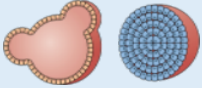
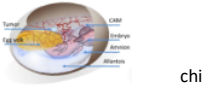






Table 4

suitability for visualizing:	Biogenesis	Secretion	Transfer	Bio-distribution	Uptake	Functional cargo transfer	Sub-cellular resolution	Relevance to human	Cost	Throughput	Key references
<b>Model system</b>											
 in vitro (2D)	++	++	-	-	+	+	++	-/+	low	high	
 in vitro (3D, e.g. organoids)	+	+	-/+	-	+	+	++	++	low	high	
 chicken chorioallantoic membrane	+	+	+	-/+	+	++	++	+	low	medium/low	
 <i>C. elegans</i>	+	+	+	+	++	++	++	-/+	low	medium	
 <i>D. melanogaster</i>	+	+	+	+	++	++	++	-/+	low	medium	
 <i>D. rerio</i>	+	+	++	++	++	++	++	+	medium	medium	
 <i>M. musculus, R. norvegicus</i>	-	-/+	+	++	+	++	o/+	++	high	low	
Image credits: Biorender, Fazio et al Nat Rev Canc 2020   References will be added to various typical applications from literature											



